Measurement report: Source apportionment of carbonaceous aerosol using dual-carbon isotopes (^{13}C and ^{14}C) and levoglucosan in three northern Chinese cities during 2018–2019

Huiyizhe Zhao [a, c, d], Zhenchuan Niu [a, b, c, d, e, *], Weijian Zhou [a, b, c, d, *], Sen Wang[f], Xue Feng[g], Shugang Wu [a, c], Xuefeng Lu [a, c], Hua Du [a, c]

[a] *State Key Laboratory of Loess and Quaternary Geology, CAS Center for Excellence in Quaternary Science and Global Change, Institute of Earth Environment, Chinese Academy of Sciences, Xi'an 710061, China*

[b] *Open Studio for Oceanic-Continental Climate and Environment Changes, Pilot National Laboratory for Marine Science and Technology (Qingdao), Qingdao 266061, China*

[c] *Shaanxi Provincial Key Laboratory of Accelerator Mass Spectrometry Technology and Application, Joint Xi'an AMS Center between IEECAS and Xi'an Jiaotong University, Xi'an 710061, China*

[d] *University of Chinese Academy of Sciences, Beijing 100049, China*

[e] *Shaanxi Guanzhong Plain Ecological Environment Change and Comprehensive Treatment National Observation and Research Station, Xi'an, China*

[f] *Shaanxi Key Laboratory of Earth Surface System and Environmental Carrying Capacity, College of Urban and Environmental Sciences, Northwest University, Xi'an, China*

[g] *Xi'an Institute for Innovative Earth Environment Research, Xi'an, China*

Correspondence: Zhenchuan Niu (niuzc@ieecas.cn) and Weijian Zhou (weijian@loess.llqg.ac.cn)

Abstract

To investigate the characteristics and changes in the sources of carbonaceous aerosols in northern Chinese cities after the implementation of the Action Plan for Air Pollution Prevention and Control in 2013, we collected $PM_{2.5}$ samples from three representative inland cities, viz. Beijing (BJ), Xi'an (XA), and Linfen (LF) from January 2018 to April 2019. Elemental carbon (EC), organic carbon (OC), levoglucosan, stable carbon isotope, and radiocarbon were measured in $PM_{2.5}$ to quantify the sources of carbonaceous aerosol, combined with Latin hypercube sampling. The best estimate of source apportionment showed that the emissions from liquid fossil fuels contributed 29.3 ± 12.7%, 24.9 ± 18.0%, and 20.9 ± 12.3% of the total carbon (TC) in BJ, XA, and LF, respectively, whereas coal combustion contributed 15.5 ± 8.8%, 20.9 ± 18.0%, and 42.9 ± 19.4%, respectively. Non-fossil sources accounted for 55 ± 11%, 54 ± 10%, and 36 ± 14% of the TC in BJ, XA, and LF, respectively. In XA, 44.8 ± 26.8% of non-fossil sources was attributed to biomass burning. The highest contributors to OC in LF and XA were fossil sources (74.2 ± 9.6% and 43.2 ± 10.8%, respectively), whereas that in BJ was non-fossil sources (66.8 ± 13.9%). The main contributors to EC were fossil sources, accounting for 91.4 ± 7.5%, 66.8 ± 23.8%, and 88.4 ± 10.8% in BJ, XA, and LF, respectively. The decline (6–16%) in fossil source contributions in BJ since the implementation of the Action Plan indicates the effectiveness of air quality management. We suggest that specific measures targeted to coal combustion, biomass burning and vehicle emissions in different cities should be strengthened in the future.

Keywords: carbonaceous aerosols; radiocarbon; stable carbon isotope; biomass burning; fossil fuel combustion; source apportionment

1 Introduction

Atmospheric aerosols are extremely complex suspension systems. Carbonaceous aerosols are an important component of atmospheric aerosols, accounting for approximately 10–60% of the total mass of global fine particulate matter (Cao et al., 2003, 2007; Feng et al., 2009). Carbonaceous aerosols contain elemental carbon (EC), organic carbon (OC), and inorganic carbon (IC). IC is mainly derived from sand dust, it has a low concentration and simple composition, and it can be removed via acid treatment (Clarke et al., 1992). EC is produced by incomplete combustion and is directly discharged from pollution sources. It can cause global warming by changing the radiative forcing and ice albedo (Jacobson et al., 2001; Kiehl et al., 2007). OC is a complex mixture of primary and secondary pollutants produced by the combustion of domestic biomass and fossil fuels. It is an important contributor to tropospheric ozone, photochemical smog, and rainwater acidification, and it can significantly impact regional and global environments through biogeochemical cycling (Jacobson et al., 2000; Seinfeld et al., 1998). Therefore, identifying and quantifying the source contributions of carbonaceous aerosols can provide a scientific basis for the management of regional air quality.

The natural radiocarbon (^{14}C) is completely depleted in fossil emissions, due to the age of fossil fuels well above the half-life of ^{14}C (5730 years), whereas non-fossil sources show the similar ^{14}C as environment (Szidat, 2009; Heal, 2014). Therefore, ^{14}C can be used to study the source of atmospheric particulate matter and to quantitatively and accurately distinguish the contributions of fossil and non-fossil sources (Clayton et al., 1955; Currie, 2000; Szidat, 2009). In recent decades, this method has been widely used to trace non-fossil carbonaceous aerosols in various regions (Ceburnis et al., 2011; Lewis et al., 2004; Szidat et al., 2009; Vonwiller et al.,

2017; Yang et al., 2005; Zhang et al., 2012, 2017a). Stable carbon isotope (^{13}C) is a useful geochemical marker that can provide valuable information about both the sources and atmospheric processing of carbonaceous aerosols (López-Veneroni, 2009; Widory, 2006), and it has been applied in various types of environmental research to identify emission sources (Cachier et al., 1985, 1986; Cao et al., 2011; Chesselet et al., 1981; Fang et al., 2017; Kawashima & Haneishi, 2012; Kirillova et al., 2013). The analysis of $^{13}C/^{12}C$ can refine ^{14}C source apportionment because both coal and liquid fossil fuels are depleted of ^{14}C while their ^{13}C source signatures are different (Andersson et al., 2015; Li et al., 2016; Winiger et al., 2017). Levoglucosan (Lev), a thermal degradation product of cellulose combustion, is a common molecular tracer that can be used to evaluate the contribution of biomass burning (Hoffmann et al., 2010; Locker et al., 1988; Simoneit et al., 1999). The combination of the carbon isotope analysis and Lev can further divide the contributions of different carbonaceous sources. Some studies have confirmed the feasibility of this combination (Claeys et al., 2010; Gelencsér et al., 2007; Genberg et al., 2011; Huang et al., 2014; Kumagai et al., 2010; Liu et al., 2013; Niu et al., 2013; Zhang et al., 2015).

Cities in northern China have been affected by severe haze for several decades (Cao et al., 2012; Han et al., 2016; Sun et al., 2006; Wang et al., 1990). After the Action Plan for Air Pollution Prevention and Control (hereafter simplified as "Action Plan") was promulgated in 2013, all parts of China responded to the issue and held numerous air quality management practices (CSC, 2013). In 2020, the average $PM_{2.5}$ concentration in Chinese cities across the country decreased by 54.2% compared to that in 2013 (MEE, 2014, 2021). In 2020, the proportion of clean energy consumption, such as that of natural gas and electricity, increased by 7.9% compared to that in 2013,

and the proportion of coal combustion decreased by 9.7% (NBS, 2021). Before the Action Plan, fossil fuel sources were identified as the main contributor to carbonaceous aerosols in Chinese cities (56–81%) (Ni et al., 2018, Niu et al., 2013, Shao et al., 1996; Sun et al., 2012; Yang et al., 2005). In this study, we aimed to determine the main contribution of the current carbonaceous aerosols in northern Chinese cities. Also, we aimed to identify whether changes in energy type and emission control caused a change in the source of carbonaceous aerosols.

To address those issues, we conducted a source apportionment of carbonaceous aerosols based on yearly measurements of OC, EC, Lev, ^{13}C, and ^{14}C in $PM_{2.5}$, combined with Latin hypercube sampling (LHS), in three representative northern Chinese cities during 2018–2019. This study provides a comprehensive understanding of current sources of carbonaceous aerosol after the implementation of the Action Plan in Chinese cities.

2 Methods

2.1 Research sites

We selected one urban sampling site in Beijing (BJ), one in Xi'an (XA), and one in Linfen (LF) (Fig. 1). BJ is the capital of China, one of the largest megacities in the world, and the central city of the Beijing–Tianjin–Hebei economic region. It has a population of more than 20 million and has experienced serious air pollution problems in the past few decades. XA, the capital of Shaanxi Province, is the ninth-largest central city and an important city of the Northwest Economic Belt in China. It is located in a basin surrounded by mountains on three sides, where atmospheric pollutants are discharged mainly from the basin and are less affected by other urban areas (Cao et al., 2009; Shen et al., 2011). LF is located in western Shanxi Province

and is one of the representative cities in the northern air-polluted region. Shanxi Province is the center of Chinese energy production and chemical metallurgy industries; its coal production and consumption were approximately 736.81 million tons and 349.07 million tons, accounting for 27.1% and 12.4% of the Chinese total in 2019, respectively (NBS, 2020; SPBS, 2020). The air quality in LF was ranked in the worst ten in China from 2018 to 2020 (MEE, 2019, 2020, 2021). According to the pollutant data released by the National Air Quality Real-time Release Platform, Ministry of Ecology and Environment (MEE) of the People's Republic of China (http://106.37.208.233:20035/), the daily average atmospheric SO_2 concentration in LF exceeded 850 μg m^{-3} on January 4th, 2017. XA and LF heavily suffer from air pollution in the Fenwei Plain. In July 2018, the State Council issued the Three-Year Action Plan to Win the Blue Sky Defense War. This included the Fenwei Plain as one of the key areas in which to prevent and control pollution (CSC, 2018).

The first site was located in the northwest of BJ, on the rooftop of the Research Center for Eco-Environmental Sciences, Chinese Academy of Sciences (40°0′33″ N, 116°20′38″ E). The site was approximately 200 m from the road. The second site was located southwest of XA, on the rooftop of the School of Urban and Environmental Sciences in Northwest University (34°15′36″ N, 108°88′53″ E). Living quarters and teaching areas were located around these two sampling sites. The third site was located in Houma, a county-level city of LF, on the rooftop of a residential building (35°63′56″ N, 111°39′53″ E). There was no industrial pollution near each site and they were representative urban sites.

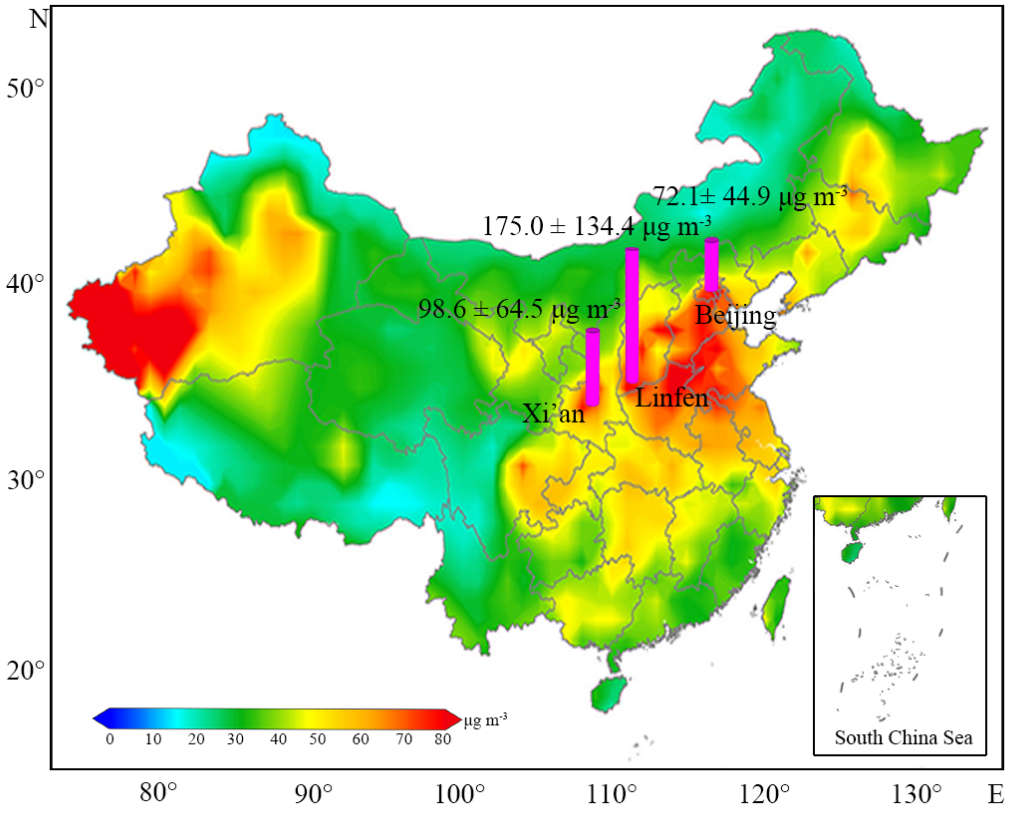

148

149 Fig. 1 Locations and $PM_{2.5}$ concentration of Beijing (BJ), Xi'an (XA), and Linfen
150 (LF). The background map shows the distribution of $PM_{2.5}$ concentrations in most of
151 China from 2015 to 2019 (Li et al., 2021a). The pink bars are the average $PM_{2.5}$
152 concentrations of the samples collected in this study during 2018 to 2019.

153

154 **2.2 Sample collection**

155 At BJ and XA, $PM_{2.5}$, samples were collected on the 7th, 14th, 21st, and 28th of
156 each month from April 28, 2018, to April 21, 2019. In LF, seven consecutive days in
157 each season were selected for sample collection, and the sampling periods were
158 concentrated in January, April, July, and October 2018. A total of 124 24-hour (10
159 a.m. to 10 a.m. on the following day) $PM_{2.5}$ samples and 4 field blanks were obtained.

160 Samples in each city were collected continuously on pre-baked quartz fiber
161 filters (203 mm × 254 mm, Whatman UK) using a high-volume (1.05 m^3 min^{-1})

sampler (TH-1000CII). The sampler was equipped with an impact collector to collect the particles less than 2.5 μm in aerodynamic diameter. To remove the existing carbon in the materials, the filter and foil used for wrapping should be baked in a muffle furnace at 375 ℃ for 5 h before use. After sampling, the filters were folded, wrapped in pre-baked aluminum foil, and stored at −18 ℃. All filters were weighed after equilibrating at 25 ± 1 ℃ and 52 ± 5% humidity for more than 24 h. The $PM_{2.5}$ mass loadings were determined gravimetrically using a 0.1 mg sensitivity electronic microbalance. Carbonate has been removed from the filters by spraying with hydrochloric acid (1 mol L^{-1}) before measurement.

2.3 OC and EC analyses

Filter pieces of 0.526 cm^2 were used to measure the OC and EC using a DRI Model 2001 (Thermal/Optical Carbon Analyzer) at the Institute of Earth Environment, Chinese Academy of Sciences. The Interagency Monitoring of Protected Visual Environments (IMPROVE) thermal/optical reflectance protocol must be followed because OC and EC have different oxidation priorities under different temperatures (Cao et al., 2007; Chow & Watson, 2002). OC and EC were defined as OC1 + OC2 + OC3 + OC4 + OP and EC1 + EC2 + EC3 − OP, respectively, in accordance with the IMPROVE protocol (Chow et al., 2004). Sample analysis results were corrected by the average blank and standard sucrose concentrations of OC and EC, respectively.

2.4 Lev analysis

The molecular tracer (Lev) was determined by high-performance anion exchange chromatography with pulsed amperometric detection (HPAEC-PAD) method at the South China Institute of Environmental Science, Ministry of Ecology and Environment. A quartz filter sample (2 cm^2) was extracted with 3 ml of deionized water in a prebaked glass bottle under ultrasonic agitation and was subsequently

analyzed using a Dionex ICS-3000 system after filtration. The separation requires an equilibrium period, isocratic elution, and gradient elution. (For a specific description, refer to Zhang et al., 2013.) The instrument sample loop was 100 μL and the detection limit of Lev was 1×10^{-8} μg ml^{-1}.

Recent studies indicated that Lev was degraded to some extent during atmospheric transportation, and about 25% of them came from other non-biomass burning sources (Hoffmann et al., 2010; Wu et al., 2021). Therefore, correction of the biomass burning source lev (Lev_{bb}) is required before the source apportionment:

$$Lev_{bb} = \frac{Lev \times 0.75}{p} \quad (1)$$

where p (0.4–0.65) is the degradation rate of Lev, which has different characteristics in each seasons. For specific p value in each season, please refer to the research of Li et al. (2021b).

2.5 Stable carbon isotope analysis

The ^{13}C compositions were determined using a gas isotopic analyzer (Picarro G2131-i) in conjunction with an elemental analyzer (Elemental Combustion System 4010) at the Institute of Earth Environment, Chinese Academy of Sciences. Specifically, 0.2–0.4 mgC of sample has been placed in a precombusted tin capsule (6×10 mm) and the air was removed by squeezing. The samples were tested at 980 ℃ and 650 ℃ with 70–80 ml min^{-1} helium as the carrier gas and 20–30 ml min^{-1} oxygen as the reaction gas. The resulting gas mixture was then collected in Gas Isotopic Analyzer (Bachar et al., 2020). Urea standard (CAS Number: 57-13-6) was used as standard sample. ^{13}C data are expressed in delta notation with respect to Vienna Pee Dee Belemnite (VPDB) (Coplen, 1996):

$$\delta^{13}C = [\frac{^{13}C/^{12}C_{Sample}}{^{13}C/^{12}C_{VPDB}} - 1] \times 1000‰ \quad (2)$$

2.6 Radiocarbon analysis

The ^{14}C samples were prepared and tested in the laboratory of Xi'an accelerator mass spectrometer (AMS) Center. The processed sample was packed in a sealed quartz tube with a silver wire and excessive CuO. The solid sample was then combusted at 850 ℃ for 2.5 h to convert it into gas after the vacuum degree was less than 5×10^{-5} mbar. The gas sample was passed through a liquid nitrogen cold trap (−196 ℃) to freeze CO_2 and water vapor, and then passed through an ethanol–liquid nitrogen cold trap (−90 ℃) to remove water vapor and purify CO_2 (Turnbull et al., 2007; Zhou et al., 2014). The collected CO_2 was reduced to graphite via a reduction reaction with zinc particles and iron powder as the reductant and catalyst, respectively (Jull, 2007; Slota et al., 1987). The graphite was pressed into an aluminum holder and measured using a 3 Megavolt AMS, with a precision of 3‰ (Zhou et al., 2006, 2007). Forty-nine targets were arranged in sequence in the sample fixed wheel, including fourty samples, six OX-II standard samples, two anthracite standard samples and one sugar carbon standard sample each time. AMS online $\delta^{13}C$ of was used for isotope fractionation correction.

The ^{14}C results were expressed as a fraction of modern carbon (f_M) (Currie, 2000; Mook & Plicht, 1999). It defines as the $^{14}C/^{12}C$ ratio of the sample related to the isotopic ratio of the reference year 1950 (Stuiver & Polach, 1977):

$$f_M = (^{14}C/^{12}C_{Sample})/(^{14}C/^{12}C_{1950}). \quad (3)$$

Atmospheric nuclear bomb tests in the late 1950s and the early 1960s released a large amount of ^{14}C, and the ratio of $^{14}C/^{12}C$ in atmospheric CO_2 roughly doubled in the mid-1960s (Hua & Barbetti, 2004; Levin et al., 2003, 2010; Lewis et al., 2004; Niu et al., 2021). However, f_M in the atmosphere has been decreasing because of the dilution effect produced by the absorption of marine and terrestrial biospheres and the

release of fossil fuels. In recent years, studies on background $^{14}CO_2$ in China and other countries have shown that the f_M value in the atmosphere has decreased and approached 1 (Hammer et al., 2017; Niu et al., 2016). This means that the impact of the nuclear explosions has almost disappeared for current atmosphere, and the change in current atmospheric ^{14}C was mainly influenced by the regional natural carbon cycle and fossil fuel CO_2 emissions. Thus, the f_M values were not corrected in this study, because the material used for biomass burning in China was mainly from crop straw (Fu et al., 2012; Street et al, 2003b; Yan et al., 2006; Zhang et al., 2017b), and the influence of atmospheric nuclear bomb test has basically vanished for the annual plants.

Non-fossil fractions (f_{nf}) and fossil fractions (f_f) were determined from the f_M values.

$$f_{nf} = f_M \times 100\% \quad (4)$$

$$f_f = (1 - f_M) \times 100\% \quad (5)$$

2.7 Source apportionment of total carbon using ^{14}C and ^{13}C

To study the contribution of each fossil source to the total carbon (TC), we used the principle of isotopic chemical mass balance to further separate fossil sources into liquid fossil fuels and coal. Since the amount of carbonaceous aerosol produced by natural gas is very low compared to coal and liquid fossil combustion, its contribution was not considered here (Chen et al., 2005; England et al., 2002; Guo et al., 2014; Yan et al., 2010). In this part, ^{13}C and ^{14}C were combined to calculate the contributions of non-fossil, coal, and liquid fossil sources.

$$f_{nf} \times \delta^{13}C_{nf} + f_{coal} \times \delta^{13}C_{coal} + f_{liq.fossil} \times \delta^{13}C_{liq.fossil} = \delta^{13}C_{sample} + \beta \quad (6)$$

$$f_{coal} + f_{liq.fossil} = f_f \quad (7)$$

where f_{nf}, f_{coal}, and $f_{liq.fossil}$ represent the proportions of non-fossil source, coal and

liquid fossil combustion, respectively, $\delta^{13}C_{nf}$, $\delta^{13}C_{coal}$, and $\delta^{13}C_{liq.fossil}$ represent $\delta^{13}C$ from the corresponding sources. $\delta^{13}C_{sample}$ is the $\delta^{13}C$ of the samples at each site, and β is a small correction.

Since the formation process of OC can cause the fractionation of ^{13}C, with a range mainly in 0.03–1.40 ‰ (mean 0.2‰) (Aggarwal and Kawamura, 2008; Cao et al, 2011; Ho et al., 2006; Zhao et al., 2018), a small correction (0.2‰) was made for the $\delta^{13}C$ sample used in Eq. 6. The selection of the reference value was described in detail in Section 2.9.

2.8 Source apportionment of OC and EC using ^{14}C and Lev_{bb}

The method combines ^{14}C with the concentration of carbon components and a molecular tracer (Lev_{bb}) to quantify the sources of OC and EC. Carbon was assumed to originate from fossil fuel combustion, biomass burning, and other non-fossil emissions (Gelencsér et al., 2007). The following is a simple calculation method.

EC consists of biomass burning (EC_{bb}) and fossil fuel combustion (EC_{ff}).

$$EC = EC_{ff} + EC_{bb} \quad (8)$$

EC_{bb} was calculated based on the Lev_{bb} concentration and the estimated EC_{bb}/Lev_{bb} ratio:

$$EC_{bb} = Lev_{bb} \times (EC_{bb}/Lev_{bb}) = Lev_{bb} \times [(EC/OC)_{bb}/(Lev_{bb}/OC_{bb})] \quad (9)$$

Then, EC_{ff} was calculated by subtraction (Eq. 8).

OC consists of OC from biomass burning (OC_{bb}), fossil fuel combustion (OC_{ff}), and other sources (OC_{other}), including primary and secondary biogenic OC and SOC (secondary organic carbon) from non-fossil emissions.

$$OC = OC_{bb} + OC_{ff} + OC_{other} \quad (10)$$

OC_{bb} was calculated based on the Lev_{bb} concentration and the estimated Lev_{bb}/OC_{bb} ratio:

$OC_{bb} = Lev_{bb}/(Lev_{bb}/OC_{bb})$ (11)

OC_{other} was calculated by balancing the ^{14}C content that was not attributed to OC_{bb}.

$OC_{other} = (OC \times f_{nf}(OC) - OC_{bb} \times f_M(bb))/ f_M(nf)$. (12)

Furthermore, $f_{nf}(OC)$ was calculated based on the ^{14}C concentration measured in the sample (detailed description of the formulas can be found in Genberg et al., 2011); $f_M(bb)$ and $f_M(nf)$ are the ^{14}C concentrations in biomass burning and other non-fossil emissions, respectively.

Finally, OC_{ff} was calculated by subtraction (Eq. 10).

2.9 Uncertainties of source apportionment

Some uncertainties exist in some parameters in Eqs. 5–11 and need to be evaluated. Table 1 lists the range of reference values used in this study. The ratios Lev_{bb}/OC_{bb} and EC_{bb}/OC_{bb} depend on the type of biofuel and the burning conditions (Oros et al., 2001a, b). In foreign studies, the most common distributions of Lev_{bb}/OC_{bb} and EC_{bb}/OC_{bb} are 0.08–0.2 and 0.07–0.45, respectively (Gelencsér et al., 2007; Puxbaumet et al., 2007; Szidat et al., 2006). The distribution ranges of Lev_{bb}/OC_{bb} and EC_{bb}/OC_{bb} burned by trees, shrubs, and rice are approximately 0.01–0.04 and 0.05–0.31, respectively (Engling et al., 2006, 2009; Wang et al., 2009). Zhang et al. (2007) found that the values of Lev_{bb}/OC_{bb} and EC_{bb}/OC_{bb} in the cereal straw of BJ were 0.08 and 0.13, respectively.

The $\delta^{13}C$ of aerosols derived from liquid fossil fuels (gasoline and diesel oil) was approximately −31 ‰ to −25 ‰ (Agnihotri et al., 2011; Huang et al., 2006; Lopez-Veneroni, 2009; Pugliese et al., 2017; Vardag et al., 2015; Widory, 2006). The $\delta^{13}C$ derived from coal combustion was relatively high, ranging from −25 ‰ to −21 ‰ (Agnihotri et al., 2011; Pugliese et al., 2017; Widory, 2006). The results of Agnihotri

et al. (2011) showed that the $\delta^{13}C$ characteristic of biomass burning emissions ranged from −25.9 ‰ to −29.4 ‰. Smith & Epstein (1971) found that plants with C3 (e.g., wheat, soybeans, and most woody plants) and C4 (e.g., corn, grass, and sugar cane) metabolism had significantly different $\delta^{13}C$, with an average of −27 ‰ and −13 ‰, respectively. In other studies, these two types of plant-derived aerosols had different characteristics; the ^{13}C from C3 and C4 plants ranged from approximately −23.9 ‰ to −32 ‰ (Moura et al., 2008; Turekian et al., 1998) and from −11.5‰ to −13.5 ‰ (Martinelli et al., 2002), respectively.

Table 1. Values with limits of input parameters for source apportionment using Latin hypercube sampling (LHS).

Parameters	Low	Probable value	High
Lev_{bb}/OC_{bb}	0.01	0.11	0.20
EC_{bb}/OC_{bb}	0.13	0.22	0.31
$\delta^{13}C_{liq.fossil}$ (‰)	−31.00	−27.00	−25.00
$\delta^{13}C_{Coal}$ (‰)	−25.00	−22.95	−21.00
$\delta^{13}C_{nf}$ [a] (‰)	−26.00	−25.25	−24.00
$\delta^{13}C_{nf}$ [b] (‰)	−27.00	−26.50	−25.00

Agnihotri et al., 2011; Engling et al., 2006, 2009; Gelencsér et al., 2007; Huang et al., 2006; Lopez-Veneroni, 2009; Martinelli et al., 2002; Moura et al., 2008; Oros et al., 2001a, b; Puxbaumet et al., 2007; Smith & Epstein, 1971; Szidat et al., 2006; Turekian et al., 1998; Wang et al., 2009; Widory, 2006; Zhang et al., 2007.

[a] Values used in BJ/LF

[b] Values used in XA

Because of the differences in the structure of biomass fuels in different cities, we selected the $\delta^{13}C$ value based on the current status of biomass fuel used in research

regions. In China, biomass fuels mainly include crop residues, branches, and leaves, and the amount of perennial wood is quite small (Zhang et al., 2015). BJ has a small area of arable land, with low agricultural output and corn production (BJMBS, 2020). The neighboring province, Hebei, is a large agricultural province that produces a large amount of wheat and corn annually; the latter has a larger sown area (PGHP, 2020). Shanxi Province also mainly produces wheat and corn; however, the sown area of corn is more than three times that of wheat (SPBS, 2020). Agricultural production in XA and the surrounding Guanzhong area is relatively large. The agricultural structure is dominated by wheat and corn, and their sown areas are not very different (SAPBS, 2020). This shows that the $\delta^{13}C$ of agricultural straw burning in LF is likely to be higher and that in XA may be lower. Some studies considered that $\delta^{13}C$ used for quantitative mass–balance source apportionment calculations from biomass burning should mainly be defined as C3 plants (Anderson et al., 2015; Fang et al., 2017; Ni et al., 2020). Based on this information, the $\delta^{13}C$ value of biomass burning in BJ and LF was found to be approximately −26 ‰ to −24 ‰, and that in XA is likely to be from approximately −27 ‰ to −25 ‰. According to the researches about biomass burning type, perennial biomass fuel was less frequently used in China (Fu et al., 2012; Street et al, 2003b; Yan et al., 2006; Zhang et al., 2017b), the impact of nuclear explosions on ^{14}C data can be ignored, and the f_M(nf) and f_M(bb) of the local station should be close to the atmospheric value.

To evaluate the uncertainties of the quantification of source contributions, which resulted from the uncertainties of the parameters used, we used Python software to generate 3000 random variable simulations based on the LHS method (Gelencsér et al., 2007). After excluding part of the out-of-range data, the median value of the remaining simulations of each sample were considered as the best estimate. The

results of the uncertainties analysis had been discussed further in Section 3.6.

2.10 Air mass backward trajectory analysis

For Backward trajectory analysis, air-mass back trajectories from the previous 48 h were determined by using the HYbrid Single-Particle Lagrangian Integrated Trajectory (HYSPLIT) model (Draxler and Hess, 1998) at three different endpoint heights (e.g., 100 m, 500 m, and 1000 m) and a time interval of 6 h for sampling day (https://www.arl.noaa.gov/).

3 Results and discussion

3.1 Characteristics and variation of carbonaceous components

During the sampling period, the average mass concentration of $PM_{2.5}$ in BJ, XA, and LF was 72.1 ± 44.9, 98.6 ± 64.5, and 175.0 ± 134.4 μg m^{-3}, respectively. All concentrations were higher in winter and lower in summer; LF showed the highest value of 368.7 ± 75.0 μg m^{-3} in winter.

Fig. 2 shows the changes in OC and EC and their ratios at the sampling sites. The carbon components in the BJ, XA, and LF samples accounted for approximately 17.5 ± 6.0%, 21.5 ± 21.0%, and 17.8 ± 7.2% of $PM_{2.5}$, respectively. Both OC and EC were changing simultaneously and were characterized by low carbonaceous concentrations in summer (OC: 8.9 ± 3.7 μg m^{-3}; EC: 1.6 ± 0.9 μg m^{-3}) and high concentrations in winter (OC: 69.2 ± 58.9 μg m^{-3}; EC: 11.8 ± 7.9 μg m^{-3}). The average OC/EC ratios in BJ, XA, and LF were 4.0 ± 1.4, 9.0 ± 6.1, and 6.6 ± 2.0, respectively. Recent studies have shown that the average ratio of OC/EC in BJ, XA, and Shanxi Province was approximately 1.22–6.5 (Han et al., 2016; Ji et al., 2018; Wang et al., 2015; Zhao et al., 2013). Generally, secondary OC (SOC) is considered to occur when OC/EC > 2 (Castro et al., 1999; Novakov et al., 2005; Turpin & Huntzicker, 1995). Additionally,

the use of biomass fuels can also enhance the OC/EC ratio (Popovicheva et al., 2014; Rajput et al., 2011). Therefore, the high OC/EC ratio indicates that carbonaceous aerosols contained a large number of SOCs or biomass burning sources, especially in XA.

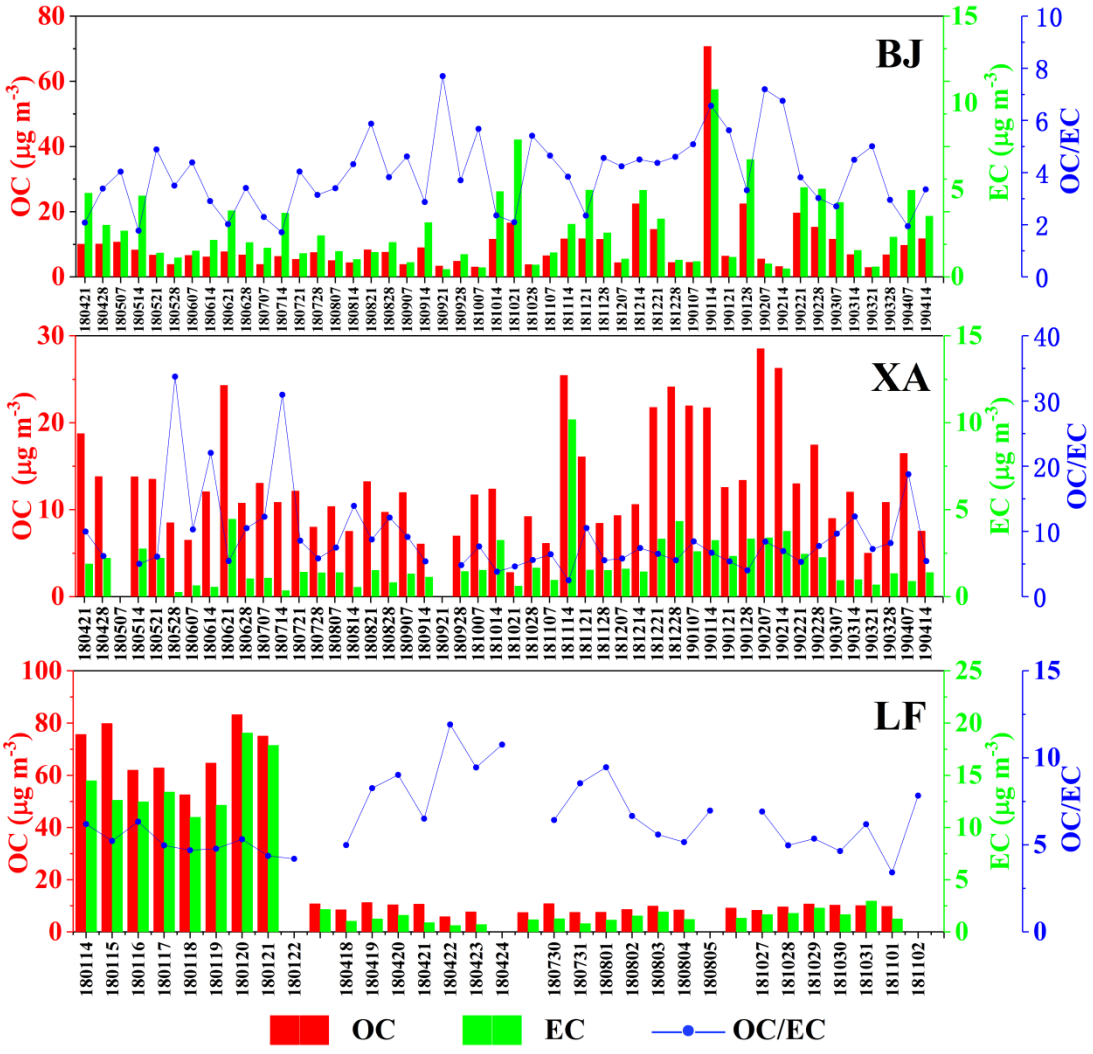

Fig. 2 Variations of elemental carbon (EC), organic carbon (OC) and their ratios in $PM_{2.5}$ at the sampling sites in Beijing (BJ), Xi'an (XA), and Linfen (LF) (date, "yymmdd").

The average mass concentrations of TC, OC, and EC at the sampling site in BJ were 12.5 ± 11.8, 9.7 ± 10.0, and 2.8 ± 2.1 μgC m^{-3}. The concentration of carbon components was relatively stable in spring and summer but fluctuated greatly in autumn and winter. The concentration of carbon components in most cases was close

to that of other periods, but there was a rapid increase in autumn and winter. The highest TC value was observed in the middle of January 2019 (81.5 μgC m^{-3}).

The average concentrations of TC, OC, and EC in XA were 14.6 ± 7.5, 12.8 ± 6.3, and 1.9 ± 1.6 μgC m^{-3}, respectively. In contrast to that in BJ, the concentration of the carbon components in XA fluctuated greatly throughout the year. Specifically, the concentration was lower from July to October and significantly higher from December to February. However, there were high concentrations of TC on some days in spring and summer, such as June 21, 2018, with the concentration reaching 28.8 μgC m^{-3}.

The average concentrations of TC, OC, and EC in LF were 35.7 ± 36.5, 30.0 ± 30.4, and 5.6 ± 6.2 μgC m^{-3}, respectively. In contrast to those in BJ and XA, the concentration of the carbon components in LF was persistently high in winter and stable and low in other seasons.

3.2 Variations of ^{14}C

The ^{14}C results showed that the average f_{nf} values in BJ, XA, and LF were 54 ± 11%, 54 ± 10%, and 36 ± 14%, respectively. Non-fossil sources were the main contributors in the BJ and XA samples (Fig. 3). Furthermore, the f_{nf} in the BJ samples showed a higher average value in spring (59 ± 6%), whereas that in the XA samples had higher average values in autumn (f_{nf}, 59 ± 7%) and winter (f_{nf}, 63 ± 6%). In the LF samples, fossil sources were the main contributors, contributing 81 ± 1% in winter.

By analyzing the f_{nf} characteristics of samples with different pollution levels based on the $PM_{2.5}$ concentration, we can study the causes and characteristics of air pollution more effectively. Using the relevant classification index of the daily average

$PM_{2.5}$ concentration in the Technical Regulation on Ambient Air Quality Index (MEE, 2012), we divided the samples into clean (with a concentration of less than 75 μg m^{-3}), regular (with a concentration between 75 and 150 μg m^{-3}), and polluted (with a concentration greater than 150 μg m^{-3}). The f_{nf} value in most samples in BJ (44 ± 8%) and LF (19 ± 2%) was lower during serious air pollution (Fig. 4), indicating that the high concentrations of aerosols in BJ and LF were more affected by fossil sources. One BJ sample had a low f_{nf} value (36%) in January and another had a high f_{nf} value (89%) in February. These samples were collected when the atmosphere was severely polluted and very clean, respectively. This might indicate that emissions from fossil fuel sources are a decisive factor of air pollution in BJ. In the XA samples, when the atmosphere was clean, f_{nf} decreased by 2–3%, indicating that the carbonaceous aerosol pollution may be more affected by biomass burning or secondary non-fossil sources from local emissions.

As can be seen in Fig. 5, the contribution of fossil sources in BJ decreased by about 6-15% for the different sampling season/period after the implementation of Action Plan, based on previous studies (Fang et al., 2017; Lim et al., 2020; Liu et al., 2016a, b; Ni et al., 2018, 2020; Shao et al., 1996; Sun et al., 2012; Yang et al., 2005; Zhang et al., 2015, 2017a) and this study. Among them, fossil sources decreased significantly in autumn and winter after the Action Plan, which were 15% and 14%, respectively. The contribution of fossil sources in our study decreased by 16% in winter compared with the previous results. For the polluted and clean periods, the proportion of fossil sources reduced by 6% and 9%, respectively. With the implementation of energy conservation and emission reduction policies, many non-clean fossil fuels have been replaced by clean energy. In 2019, the coal

consumption in BJ was only 1.3 million tons, which was 91.5% lower than that in 2013 (BJMBS, 2020).

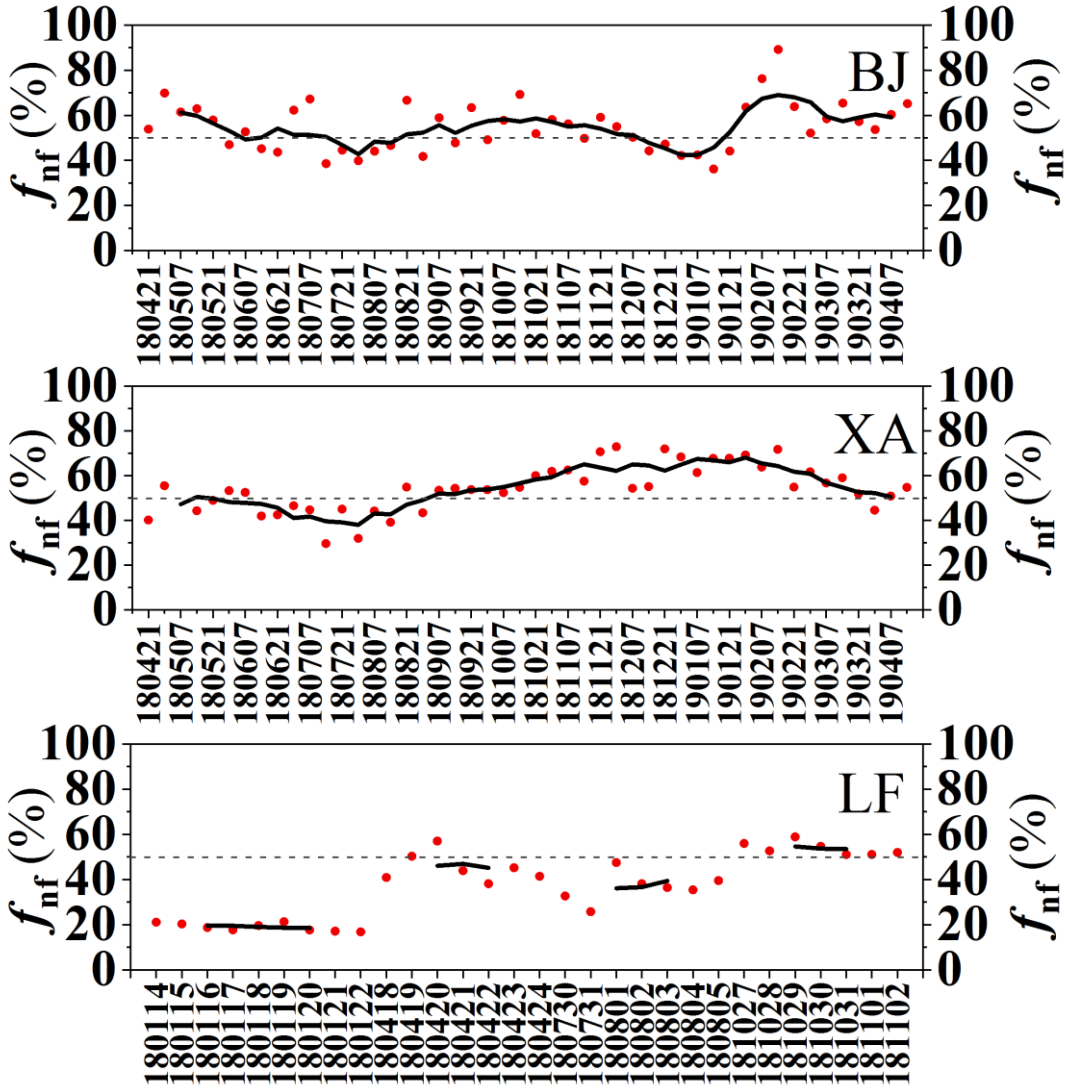

Fig. 3 Variations in proportion of non-fossil sources (f_{nf}) of carbonaceous aerosols at the sampling sites in Beijing (BJ), Xi'an (XA), and Linfen (LF). The red scatter dot represents the f_{nf} of each sample, and the black solid line represents the sliding average f_{nf} value of every five samples (date, "yymmdd").

Different from the results in BJ, the proportion of fossil sources in XA has not decreased significantly for each season/period (Fig. 5). This difference might be related with a small decline (< 0.5%) in coal consumption in Xi'an during 2019 compared to 2013 (XAMBS, 2014, 2020). Due to the less attention to LF, there is still

a lack of related research of carbonaceous aerosols using radiocarbon in this city to compare.

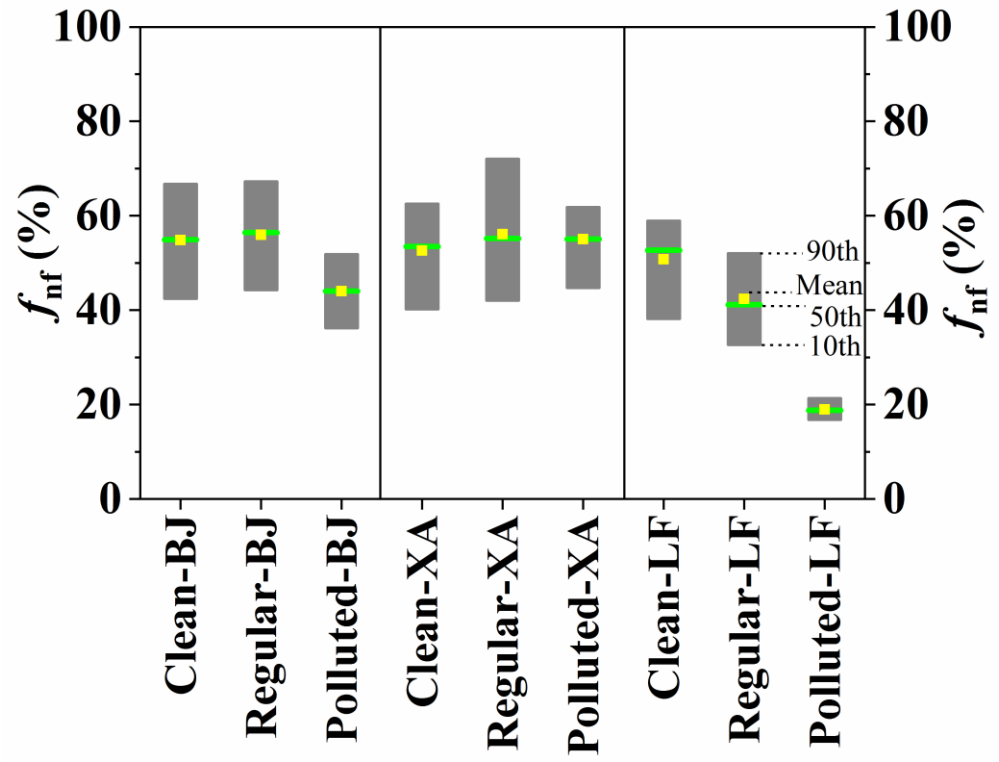

Fig. 4 Boxplot distribution of f_{nf} of samples with different pollution levels. Clean samples: $PM_{2.5} < 75$ μg m^{-3}; regular samples: 75 μg $m^{-3} \leq PM_{2.5} < 150$ μg m^{-3}; polluted samples: $PM_{2.5} \geq 150$ μg m^{-3}.

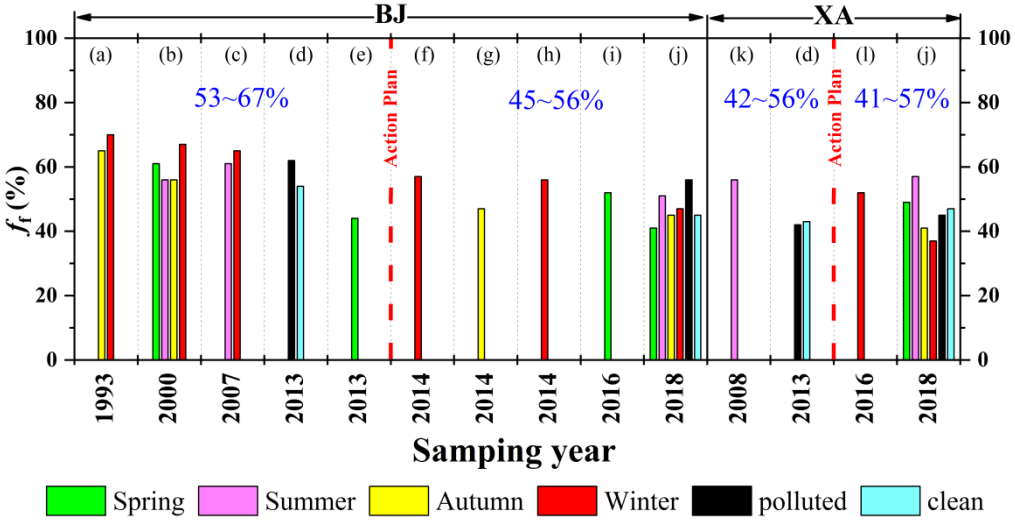

Fig. 5 Comparison of fossil proportion (f_f) of carbonaceous aerosol reported in different studies in Beijing (BJ) and Xi'an (XA), China for each season/period. The

data has been converted to the ratio of total carbon. The ranges shown in the upper part of the figure are the average values of each season/period before and after the Action Plan. (a) Shao et al., 1996; (b) Yang et al., 2005; (c) Sun et al., 2012; (d) Zhang et al., 2015; (e) Liu et al., 2016b; (f) Zhang et al., 2017; (g) Liu et al., 2016a; (h) Fang et al, 2017; (i) Lim et al., 2020; (j)This study; (k) Ni et al., 2018; (l) Ni et al., 2021.

3.3 Air mass backward trajectory analysis

We analyzed and counted the backward trajectory during the sampling period; several typical types were presented in Fig. S1. Figure S1 (a) shows the type of backward trajectory with the highest frequency during the sample collection in BJ. This type of long-distance transportation from the northwest accounted for approximately 43.9% of all cases. The average $PM_{2.5}$ concentration, carbonaceous aerosol concentration, and f_{nf} of the sample were 45.4 ± 22.7 μg m^{-3}, 9.5 ± 6.4 μgC m^{-3}, and 56 ± 10%, respectively. As shown in Fig. S1 (b), when air mass was transported from the south or stayed for a long time in the Hebei province, air pollution was usually more serious. These cases accounted for approximately 26.3% of all cases. The average concentrations of $PM_{2.5}$ and carbonaceous aerosols were 97.3 ± 43.6 μg m^{-3} and 15.6 ± 7.9 μgC m^{-3}, which were 2.1 and 1.6 times of those in the northwest, respectively. The aerosol concentration of air masses transported from the southern region was higher than that from the northern regions. The f_{nf} value in these cases was 46 ± 5%, which was 10% higher than in the northwest cases. Thus, air pollution in BJ might be affected by fossil sources in the Hebei province and other southern regions.

The $PM_{2.5}$ and carbonaceous concentrations were low when the air mass transported from the northwest for a long distance at the XA site (Fig. S1 (c)). In this case, the average $PM_{2.5}$ concentration, carbonaceous aerosol concentration, and f_{nf} of the samples were 93.1 ± 65.1 μg m^{-3}, 17.4 ± 9.6 μgC m^{-3}, and 62 ± 7%, respectively. However, when air masses circulated in the Guanzhong Basin or converged into the basin from multiple directions due to the local topography (Fig. S1 (d)), the concentration of carbonaceous aerosol was usually high. The proportion of this type of air mass transportation accounted for 53.6% of the total cases. The average $PM_{2.5}$ concentration, carbonaceous aerosol concentration, and f_{nf} of the corresponding samples were 132.0 ± 72.8 μg m^{-3}, 19.7 ± 10.4 μgC m^{-3}, and 58 ± 9%, respectively. Thus, air pollution in XA was mainly affected by the diffusion environment. The air mass remained in the upper part of the Guanzhong region for a long time when the diffusion environment was poor, causing secondary reactions and air pollution. Moreover, when the air mass came from eastern cities (e.g., Henan or Hubei provinces), f_{nf} was 47%, which was significantly lower than that in other cases. This indicated that fossil source emissions in Henan and other eastern regions might contribute to air pollution in XA.

As shown in Fig. S1 (e), when the air mass was long-distance transported to the LF, the concentration of carbonaceous aerosols was relatively stable. However, pollutants accumulated when the air mass returned over and around the city (Fig. S1 (f)). In these cases, the concentrations of $PM_{2.5}$ and carbonaceous aerosols of the sample increased by 46.35–57.10%, and f_{nf} decreased by 5%. Thus, the LF samples were more susceptible to the diffusion environment and the proportion of fossil sources discharged locally.

Air pollution in BJ was more susceptible to the impact of transportation from the southern region, whereas XA and LF were more affected by local emissions and diffusion environments.

3.4 Best estimate of source apportionment of TC using ^{14}C and ^{13}C

The $\delta^{13}C$ values at the sampling sites in BJ, XA, and LF were −25.65 ± 0.79‰, −26.94 ± 0.92‰, and −23.84 ± 0.16‰, respectively. Figure 6 shows the $\delta^{13}C$ values of the samples from each city and various sources. Specifically, $\delta^{13}C$ had lower values in the BJ and LF samples during summer (−26.11 ± 0.49‰ and −24.88 ± 0.18‰, respectively) and higher values during winter (−25.07 ± 0.79‰ and −23.84 ± 0.16‰, respectively). Conversely, the lower and higher $\delta^{13}C$ values in the XA samples appeared in winter (−27.49 ± 0.44‰) and spring (−26.34 ± 1.23‰).

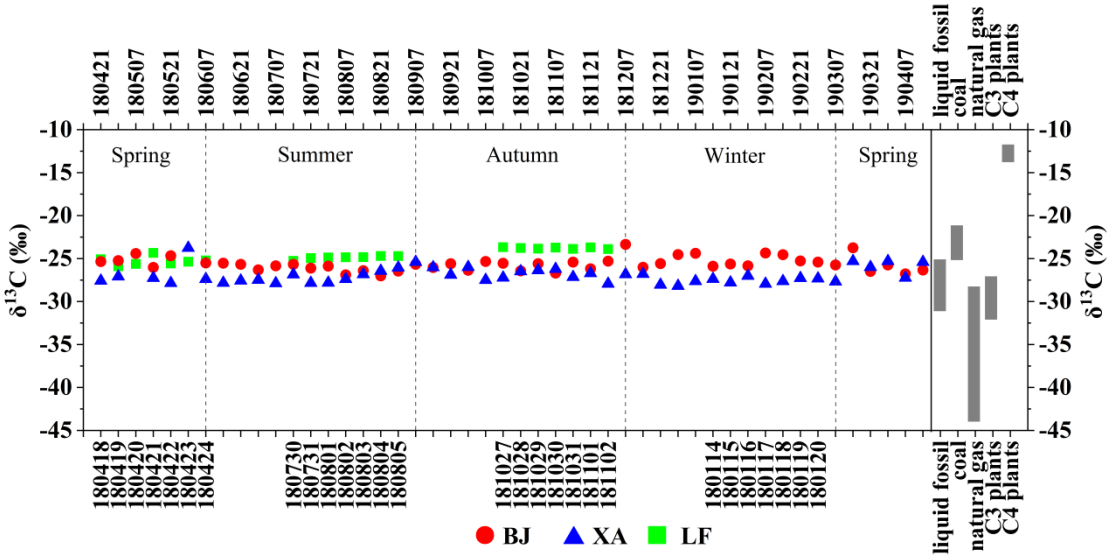

Fig. 6 $\delta^{13}C$ values of samples from Beijing (BJ), Xi'an (XA), and Linfen (LF), and comparison with the $\delta^{13}C$ distribution of various sources. The abscissa represents the sampling date (yymmdd). The tick labels of top axis represent the date of BJ and XA, and the bottom represents the date of LF. The gray box indicates the $\delta^{13}C$ of the main source (Agnihotri et al., 2011; Huang et al., 2006; Lopez-Veneroni, 2009; Martinelli

et al., 2002; Moura et al., 2008; Pugliese et al., 2017; Smith & Epstein, 1971; Vardag et al., 2015; Widory, 2006).

Compared with the existing isotope indicators of various sources (Fig. 6), the increase in $\delta^{13}C$ in the BJ and LF samples during winter may be more related to the increase in coal combustion from local and the surrounding cities. The increase in $\delta^{13}C$ in XA samples during autumn and winter may be related to the use of C4 plant fuel, whereas the decrease during winter may be related to vehicle emissions and the use of C3 plant fuels, such as wheat straw or wood.

^{14}C and ^{13}C were used to quantify the sources of TC in the carbonaceous aerosols (Fig. 7). For the carbonaceous aerosols in BJ and XA, the best estimate of source apportionment showed that the contributions of liquid fossil fuels were 29.3 ± 12.7% and 24.9 ± 18.0%, respectively, which were greater than the contribution of coal (15.5 ± 8.8% and 20.9 ± 14.2%, respectively). In 2019, coal accounted for only 2.6% of all fossil fuels used in BJ (BJMBS, 2020). This indicates that the local combustion of coal was very low, and the coal contribution might be somewhat related to transportation from the surrounding regions. Moreover, the higher contribution of liquid fossil fuels in BJ was due to the high number of motor vehicles (6.4 million), which was 1.7 times higher than that in XA in 2019(BJMBS, 2020; XAMBS, 2020). Figure S2 shows some studies on the source apportionment of coal and liquid fossil fuels in aerosols in BJ over the past few decades. The coal contribution in BJ decreased, whereas liquid fossil fuels gradually became the main source of fossil fuels. After the implementation of the Action Plan, the proportion of coal in fossil sources decreased by approximately 32% in BJ (Gao et al., 2018; Li et al., 2013; Liu et al., 2014; Shang et al., 2019; Song et al., 2006; Tian et al., 2016; Wang et al., 2008; Zhang et al., 2014).

In contrast, coal combustion contributed 42.9 ± 19.4% to LF samples, which was greater than the contribution of liquid fossil emissions (20.9 ± 12.3%) and significantly higher than those in BJ and XA. Especially in winter, coal contributed as much as 68.6 ± 3.6% (59.1 ± 10.0 μgC m^{-3}). According to the data released by the Shanxi Provincial Bureau of Statistics, coal consumption in Shanxi Province was as high as 349.06 million tons in 2019, which was 46.7 times of the consumption of liquid fossil fuels, accounting for 70.3% of the total fossil fuel consumption (SPBS, 2020). The high contribution of coal combustion in winter might be related to the use of household coal for heating by rural residents in Shanxi. This is because household coal can emit a large amount of carbonaceous particles and is an important source of carbonaceous aerosols in rural areas in northern China (Chen et al., 2005; Shen et al., 2010; Streets et al., 2003a; Zhi et al., 2008).

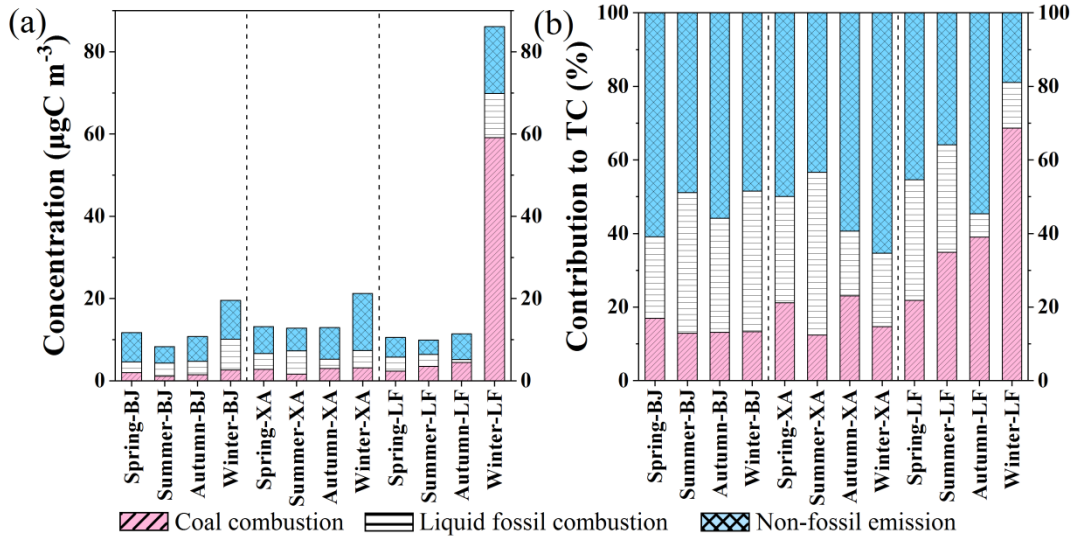

Fig. 7 Mass concentrations (μgC m^{-3}) (a) and percentage (b) of coal combustion, liquid fossil fuel, and non-fossil sources emissions for carbonaceous aerosols samples in Beijing (BJ), Xi'an (XA), and Linfen (LF) during different seasons.

3.5 Best estimate of source apportionment of OC and EC by ^{14}C and Lev

The concentration of each carbon component in BJ, XA, and LF was calculated based on the combination of Lev and ^{14}C. The best estimate of source apportionment showed in Fig. 8. The contributions of OC_{other} (43.6 ± 12.9%), OC_{ff} (25.5 ± 11.7%), and EC_{ff} (20.5 ± 6.5%) were relatively high in BJ. The OC_{bb} (23.0 ± 17.3%) and OC_{ff} (39.7 ± 9.7%) were the highest contributors in XA. The LF samples showed different characteristics, and the contribution of fossil sources was significantly high, especially for the OC_{ff} (56.1 ± 11.9%).

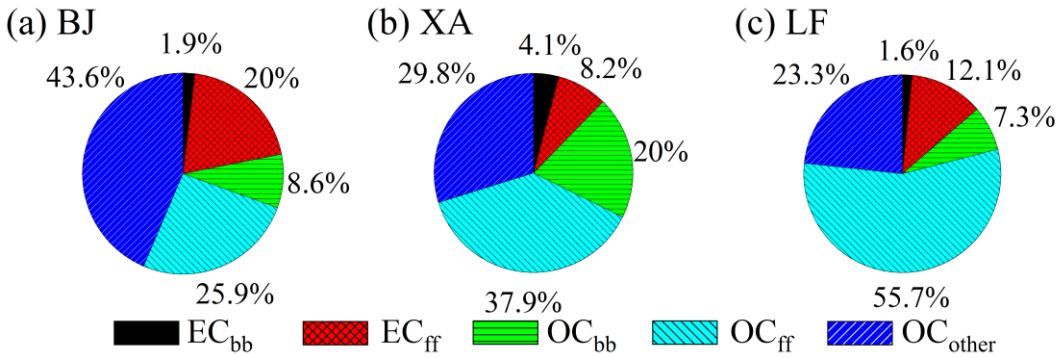

Fig. 8 Percentage of elemental carbon from biomass burning (EC_{bb}) and fossil-fuel combustion (EC_{ff}) and percentage of organic carbon from biomass burning (OC_{bb}), fossil-fuel combustion (OC_{ff}), and other sources (OC_{other}) for the $PM_{2.5}$ samples in Beijing (BJ), Xi'an (XA), and Linfen (LF).

3.5.1 Biomass burning contribution to TC

The concentrations (0.3 ± 0.3 μgC m^{-3}) and contributions (1.9 ± 1.4%) of EC_{bb} in BJ were relatively low during the whole year (Fig. 9). The EC_{bb} at the XA and LF sites had high concentrations in autumn (0.7 ± 0.5 μgC m^{-3} and 0.6 ± 0.1 μgC m^{-3}) and winter (1.5 ± 0.7 μgC m^{-3} and 1.7 ± 0.3 μgC m^{-3}) and low concentrations in summer (0.2 ± 0.1 μgC m^{-3} and 0.1 ± 0.0 μgC m^{-3}), respectively. The OC_{bb} concentrations in the BJ, XA, and LF samples showed an increase in autumn (1.6 ± 1.4 μgC m^{-3}, 3.3 ± 2.2 μgC m^{-3}, and 2.9 ± 0.4 μgC m^{-3}) and winter (2.5 ± 2.1 μgC m^{-3}, 6.9 ± 3.3 μgC m^{-3}, and 7.9 ± 1.3 μgC m^{-3}), respectively. Especially in the XA samples, OC_{bb} had high

582 contributions in autumn (28.6 ± 15.8%) and winter (32.8 ± 12.3%). The contribution
583 of biomass combustion in XA (24.1 ± 18.0%) was significantly larger than that in BJ
584 (10.8 ± 7.9%) and LF (8.8 ± 8.9%), which was also reflected in the concentration of
585 Lev (Fig. S3). The Lev concentration in XA (0.36 ± 0.38 μg m^{-3}) was higher than that
586 in BJ (0.15 ± 0.17 μg m^{-3}) and slightly higher than that in LF (0.32 ± 0.34 μg m^{-3}).
587 Furthermore, the Lev concentration in XA during autumn and winter was up to 5.3
588 times higher than that during the other seasons. Especially in winter, the proportion of
589 Lev in the TC was 4.0 ± 2.3% in XA, which was 3.9 and 3.8 times those in BJ and LF,
590 respectively. Zhang et al. (2015) attributed this to emissions from neighboring rural
591 regions because such areas use biofuels for heating and cooking more commonly in
592 winter. China produces 939 million tons of agricultural biomass residues annually,
593 which is the main energy source for some rural areas (Liao et al., 2004; Lu et al.,
594 2009). In addition, the increase in urban vegetation coverage may also increase the
595 photochemical reactions of biological volatile organic compounds (VOCs) (Gelencsér
596 et al., 2007; NBS, 2021). Therefore, in recent years, non-fossil fuels have gradually
597 become a major contributor to carbonaceous aerosols in BJ and XA with the reduction
598 in the use of fossil energy.

599 **3.5.2 Fossil contribution to TC**

600 The EC_{ff} concentrations at BJ (spring: 2.7 ± 1.4 μgC m^{-3}; summer: 2.0 ± 0.8 μgC
601 m^{-3}; autumn: 2.3 ± 2.0 μgC m^{-3}; winter: 2.9 ± 2.6 μgC m^{-3}) and XA (spring: 1.1 ± 0.8
602 μgC m^{-3}; summer: 1.1 ± 1.1 μgC m^{-3}; autumn: 1.6 ± 2.3 μgC m^{-3}; winter: 1.4 ± 0.8
603 μgC m^{-3}) did not fluctuate significantly during the year. The concentration of EC_{ff} in
604 LF during spring, summer, and autumn was relatively stable (1.0–1.2 μgC m^{-3}), but it
605 was high during winter (12.5 ± 2.5 μgC m^{-3}), reaching 10.2 times that in summer.

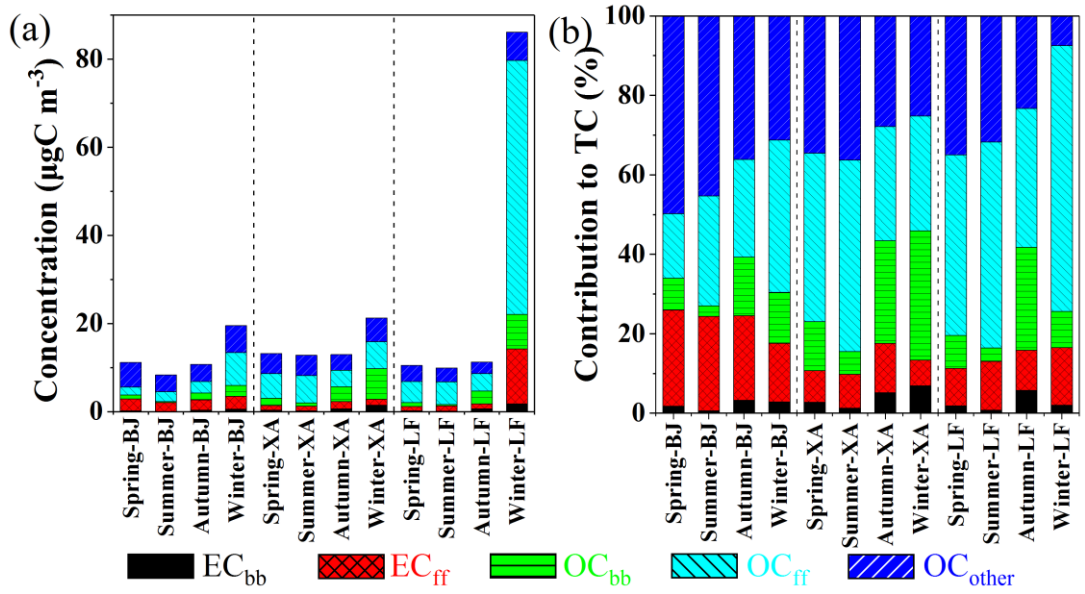

606

607 Fig. 9 Mass concentrations (μgC m^{-3}) (a) and percentage (b) of elemental carbon from
608 biomass burning (EC_{bb}) and fossil-fuel combustion (EC_{ff}), organic carbon from
609 biomass burning (OC_{bb}), fossil-fuel combustion (OC_{ff}), and other sources (OC_{other}) for
610 carbonaceous aerosols samples in Beijing (BJ), Xi'an (XA), and Linfen (LF) during
611 different seasons.

612 The concentration of OC_{ff} was slightly higher in XA during summer (6.2 ± 2.2
613 μgC m^{-3}) and winter (6.1 ± 2.1 μgC m^{-3}). The contribution of OC_{ff} in the BJ samples
614 increased to 32.4 ± 14.5% during winter and decreased to 18.4 ± 8.4% during spring.
615 The OC_{ff}/EC_{ff} ratios in BJ and LF during winter were approximately 2.3 ± 1.2 and 4.7
616 ± 0.7, respectively, suggesting that the fossil source secondary carbonaceous aerosols
617 were higher in winter. This can be explained by the lower temperature in the winter
618 altering the gas–particle equilibrium, suggesting that a larger portion of the OC_{ff}
619 during winter was secondary aerosol (Genberg et al., 2011). OC_{ff} in LF had high
620 concentrations in winter (57.6 ± 9.2 μgC m^{-3}) and low concentrations in summer (5.2
621 ± 1.2 μgC m^{-3}). This indicated that the burning of fossil sources was an important
622 source of OC in BJ (OC_{ff}: 32.4 ± 14.5%) and LF (OC_{ff}: 66.8 ± 1.7%) during winter.
623 Fang et al. (2017) found that fossil fuels contributed significantly (> 50%) to carbon

components in the haze in East Asia during January 2014, suggesting that the aerosol contribution was generally dominated by fossil combustion sources. Therefore, using cleaner energy and cleaner residential stoves to reduce and replace the high-emission end-use coal combustion processes and control the emissions from liquid-fossil-fueled vehicles in megacities should be beneficial to the air quality.

3.5.3 Other non-fossil contributions to OC

In addition to the OC directly emitted from fossil and biomass fuels, there are many components of OC, such as SOC, whose source is difficult to identify. Residential oil fume emissions from urban residents, emissions from biological sources, and secondary bio-organic aerosols generated by the secondary reaction of biomass fuels are also important components of OC (Gelencsér et al., 2007; Zhang et al., 2015).

The concentration of OC_{other} in the LF samples did not vary greatly during spring (3.7 ± 1.2 μgC m^{-3}) and summer (3.2 ± 0.5 μgC m^{-3}) but it was lower in autumn (2.6 ± 0.3 μgC m^{-3}) and higher in winter (6.5 ± 2.8 μgC m^{-3}),. In BJ, the contribution of OC_{other} was high during spring ($49.9 \pm 9.9\%$) and summer (45.8 ± 9.8 %), and its concentration was relatively high during winter (6.1 ± 5.6 μgC m^{-3}). Zhang et al. (2015) mainly attributed the presence of OC_{other} in northern China to SOC formation from non-fossil, non-biogenic precursors. In general, secondary bio-organic aerosols in spring and autumn are mainly caused by biological emissions or long-distance transportation of biological VOCs and secondary organic aerosols (SOAs) in particulates (Gelencsér et al., 2007; Jimenez et al., 2009). The high concentration in winter may be because low temperatures drive condensable semi-volatile organic compounds (SVOCs) into the particulate phase (Simpson et al., 2007; Tanarit et al., 2008).

649 The OC_{other} contribution and concentration in XA were high in summer (35.2 ±
650 10.0%) and winter (5.4 ± 4.2 μgC m^{-3}), respectively. We assume that this excess is
651 mainly attributed to SOC formation from non-fossil and primary biogenic particles.
652 Some SOAs are formed by VOCs that are produced by burning wood or biofuels (e.g.,
653 ethanol), and they increase the load of these sources on organic aerosols (Genberg et
654 al., 2011). Huang et al. (2014) found that severe haze pollution was largely driven by
655 secondary aerosol formation, and non-fossil SOAs dominated, accounting for 66 ±8%
656 of the SOAs in XA despite extensive urban emissions. Ni et al. (2020) also considered
657 that non-fossil sources largely contributed (56%) to SOC in XA. Thus, the control of
658 biomass burning activities could be an efficient strategy for reducing aerosols,
659 especially in XA. Furthermore, SOC formation from these non-fossil VOCs may be
660 enhanced when they are mixed with other pollutants, such as VOCs and NO_x (Hoyle
661 et al., 2011; Weber et al., 2007). Motor vehicles are one of the main anthropogenic
662 sources of VOCs and NO_x (Barletta et al., 2005; Liu et al., 2008). In Section 3.4, we
663 found that the carbonaceous concentrations from motor vehicle emissions were high
664 in XA during winter and summer (Fig. 7a), and the increasing of motor vehicle
665 activities might partly explain the high concentration of OC_{other} during the two
666 seasons.
667
668 **3.6 Uncertainty analysis**
669 The results of the uncertainty analysis of the given set (Table 1) of the
670 parameters in the three cities were shown in Fig. 10. Each curve represents the
671 probability distribution of the sources of carbon components that contribute to the TC,
672 from which the uncertainty of the source allocation can be derived. Some results were
673 uncertain because the input parameters of the LHS calculation varied greatly. The

674 contributions of OC_{ff} and OC_{other} to the TC were mostly uncertain. This is mainly
675 related to the uncertainty of the two parameters, Lev/OC_{bb} and $(EC/OC)_{bb}$. Both these
676 parameters depend on the burning conditions and type of biomass, as mentioned in
677 Section 2.9. More reliable data would be obtained if $^{13}C/^{14}C$ could be performed on
678 the pure OC fractions of the samples, which has been proven to be feasible (Huang et
679 al., 2014; Szidat et al., 2004, 2006; Zhang et al., 2015). Other contributions have
680 single peaks, which prove that the results of the source analysis are reliable. These
681 results demonstrate that we can identify the main contributors.

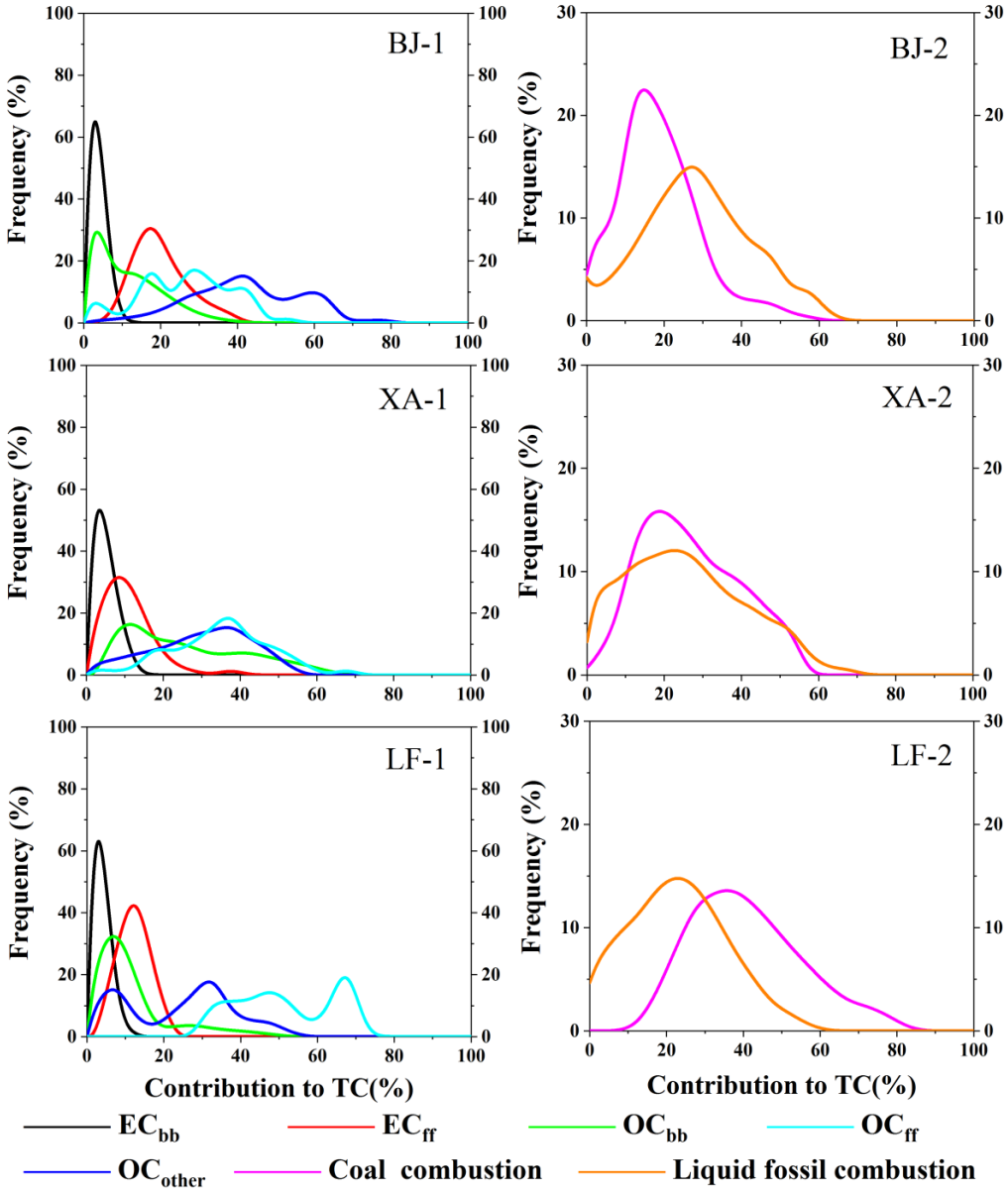

682

683 Fig. 10 Latin hypercube sampling of frequency distributions of the source
684 contributions to total carbon (TC) from fossil, organic carbon (OC), and elemental
685 carbon (EC) source categories (Table 1) for the samples collected in Beijing (BJ),
686 Xi'an (XA), and Linfen (LF).
687

688 ## 4 Conclusions

689 $PM_{2.5}$ samples were collected from BJ, XA, and LF in northern China from
690 January 2018 to April 2019. The main objective of this study was to quantify the
691 sources of carbonaceous aerosols by measuring the EC, OC, Lev, ^{13}C, and ^{14}C
692 combined with LHS.

693 The TC accounted for approximately 17.5 ± 6%, 21.5 ± 21%, and 17.8 ± 7.2% of
694 $PM_{2.5}$ in the samples from BJ, XA, and LF, and the corresponding concentrations
695 were 12.5 ± 11.8 μgC m^{-3}, 14.6 ± 7.5 μgC m^{-3}, and 35.7 ± 36.5 μgC m^{-3}, respectively.
696 The concentrations at the three sites showed high values in winter and low values in
697 summer. Based on backward trajectory analysis, we found that carbonaceous aerosols
698 in BJ were more susceptible to transportation from the southern regions. Local
699 emissions and the diffusion environment significantly impacted carbonaceous
700 aerosols in XA and LF.

701 The best estimate of source apportionment of the fossil components in the TC
702 showed that the contribution of liquid fossil fuel combustion was 29.3 ± 12.7% and
703 24.9 ± 18.0% in BJ and XA, respectively, which was greater than the contribution of
704 coal combustion (15.5 ± 8.8%; 20.9 ± 14.5%). In contrast, coal combustion
705 contributed 42.9 ± 19.4% in LF, which was greater than the contribution of liquid
706 fossil fuel combustion (20.9 ± 12.3%).

707 The best estimate of source apportionment of OC and EC indicated that the

contributions of EC_{ff} (20.0 ± 6.5%), OC_{ff} (25.9 ± 11.6%), and OC_{other} (43.6 ± 12.9%) were relatively high in BJ. The OC_{ff} contribution was higher in winter (32.4 ± 14.5%), and its concentration was 3.3 times higher than that in other seasons. The contribution of OC_{bb} (20.0 ± 15.3%) and OC_{ff} (37.9 ± 10.8%) was higher in XA. The contribution of biomass burning to the TC was as high as 39.6 ± 14.5% in winter. The contribution of OC_{ff} in LF was significantly high (55.7 ± 12.2%), especially in winter (66.8 ± 1.7%).

The decline (6–16%) in the contribution of fossil sources since the implementation of the Action Plan indicates the effectiveness of air quality management. In the future, the government needs to further regulate and control emissions from motor vehicles in megacities such as BJ and XA. The cleaner use of coal must be further strengthened in coal-based cities such as LF in the eastern part of the Fenwei Plain. This study indicates that attention should be paid to the control of biomass burning in northern China, especially in the Guanzhong region.

Code and data availability: The data products in this paper are available at the East Asian Paleoenvironmental Science Database, National Earth System Science Data Center, National Science & Technology Infrastructure of China (http://paleodata.ieecas.cn/index_EN.aspx).

Author contributions: HZ performed the data analysis and wrote the initial draft of the manuscript. ZN and WZ conceived the project and reviewed the paper. ZN and SW provided the samples. HZ, XF, SW, XL and HD conducted the measurements. All authors made substantial contributions to this work.

Competing interests: The authors declare that they have no conflict of interest.

Acknowledgments: The authors acknowledge the help of anonymous reviewers for improving this article.

Financial support: The study was financially supported by the Strategic Priority Research Program of the Chinese Academy of Sciences (XDA23010302), National Research Program for Key Issues in Air Pollution Control (DQGG0105-02), the National Natural Science Foundation of China (41730108, 42173082, and 41773141), Natural Science Foundation of Shaanxi province (2014JQ2-4018), Key projects of CAS (ZDRW-ZS-2017-6), and Natural Science Basic Research Program of Shaanxi Province (2019JCW-20).

References

Aggarwal, S. G., and Kawamura, K.: Molecular distributions and stable carbon isotopic compositions of dicarboxylic acids and related compounds in aerosols from Sapporo, Japan: Implications for photochemical aging during long-range atmospheric transport, J. Geophys. Res, 113, D14301, https://doi.org/10.1029/2007JD009365, 2008.

Agnihotri, R., Mandal, T. K., Karapurkar, S. G., Naja, M., Gadi, R., Ahammmed, Y. N., Kumar, A., Saud, T., and Saxena, M.: Stable carbon and nitrogen isotopic composition of bulk aerosols over India and northern Indian Ocean, Atmos. Environ., 45, 2828-2835, https://doi.org/10.1016/j.atmosenv.2011.03.003, 2011.

Andersson, A., Deng, J. J., Du, K., Zheng, M., Yan, C. Q., Sköld, M., and Gustafsson, O. r.: Regionally-varying combustion sources of the January 2013 severe haze

758 events over eastern China, Environ. Sci. Technol., 49, 2038-2043,
759 https://doi.org/10.1021/es503855e, 2015.
760 Bachar, A., Markus-Shi, J., Regev, L., Boaretto, E., and T. Klein, T.: Tree rings reveal
761 the adverse effect of water pumping on protected riparian Platanus orientalis tree
762 growth, For. Ecol. Manag., 458, 0378-1127,
763 https://doi.org/10.1016/j.foreco.2019.117784, 2020.
764 Barletta, B., Meinardi, S., Rowland, F. S., Chan, C., Wang, X. M., Zou, S. C., Chan,
765 L., and Blake, D. R.: Volatile organic compounds in 43 Chinese cities, Atmos.
766 Environ., 39, 5979-5990, https://doi.org/10.1016/j.atmosenv.2005.06.029, 2005.
767 BJMBS: (Beijing Municipal Bureau Statistics): Beijing Statistical Yearbook-2020,
768 China Statistics press.,
769 http://nj.tjj.beijing.gov.cn/nj/main/2020-tjnj/zk/indexch.htm, 2020 (last access:
770 28 March 2022).
771 Cachier, H., Buat Menard, P., Fontugne, M., and Rancher, J.: Source terms and source
772 strengths of the carbonaceous aerosol in the tropics, J. Atmos. Chem., 3, 469-489,
773 https://doi.org/10.1007/BF00053872, 1985.
774 Cachier, H., Buat Menard, P., Fontugne, M., and Chesselet, R.: Long‐range transport
775 of continentally-derived particulate carbon in the marine atmosphere: Evidence
776 from stable carbon isotope studies, Tellus B, 38, 161-177,
777 https://doi.org/10.1111/j.1600-0889.1986.tb00184.x, 1986.
778 Cao, J. J., Lee, S. C., Ho, K. F., Zhang, X. Y., Zou, S. C., Fung, K., Chow, J. C., and
779 Watson, J. G.: Characteristics of carbonaceous aerosol in Pearl River Delta
780 Region, China during 2001 winter period, Atmos. Environ., 37, 1451-1460,
781 https://doi.org/10.1016/S1352-2310(02)01002-6, 2003.
782 Cao, J. J., Lee, S. C., Chow, J. C., Watson, J. G., Ho, K. F., Zhang, R. J., Jin, Z. D.,

783 Shen, Z. X., Chen, G. C., and Kang, Y. M.: Spatial and seasonal distributions of
784 carbonaceous aerosols over China, Journal of Geophysical Research
785 Atmospheres, D112, 22-11, https://doi.org/10.1029/2006JD008205, 2007.
786 Cao, J. J., Zhu, C. S., Chow, J. C., Watson, J. G., Han, Y. M., Wang, G. H., Shen, Z. X.,
787 and An, Z. S.: Black carbon relationships with emissions and meteorology in
788 Xi'an, China, Atmos. Res., 94, 194-202, https://doi.org/10.1029/2006JD008205,
789 2009.
790 Cao, J. J., Chow, J. C., Tao, J., Lee, S. C., Watson, J. G., Ho, K., Wang, G. H., Zhu, C.
791 S., and Han, Y. M.: Stable carbon isotopes in aerosols from Chinese cities:
792 Influence of fossil fuels, Atmos. Environ.,
793 https://doi.org/10.1016/j.atmosenv.2010.10.056, 2011.
794 Cao, J. J., Shen, Z. X., Chow, J. C., Watson, J. G., Lee, S. C., Tie, X. X., Ho, K. F.,
795 Wang, G. H., and Han, Y. M.: Winter and summer PM2.5 chemical compositions
796 in fourteen Chinese Cities, Air Waste Manage Assoc, 62, 1214–1226,
797 https://doi.org/10.1080/10962247.2012.701193, 2012.
798 Castro, L. M., Pio, C. A., Harrison, R. M., and Smith, D.: Carbonaceous aerosol in
799 urban and rural European atmospheres: estimation of secondary organic carbon
800 concentrations, Atmos. Environ., 33, 2771-2781,
801 https://doi.org/10.1111/j.1553-2712.2005.tb00860.x, 1999.
802 Ceburnis, D., Garbaras, A., Szidat, S., Rinaldi, M., Fahrni, S., Perron, N., Wacker, L.,
803 Leinert, S., Remeikis, V., Facchini, M. C., Prevot, A. S. H., Jennings, S. G., and
804 O'Dowd, C. D.: Quantification of the carbonaceous matter origin in submicron
805 marine aerosol particles by dual carbon isotope analysis, Atmos. Chem. Phys.
806 Discuss., 11, 8593-8606, https://doi.org/10.5194/acpd-11-2749-2011, 2011.
807 Chen, Y. J., Sheng, G. Y., Bi, X. H., Feng, Y. L., Mai, B. X., and Fu, J. M.: Emission

Factors for Carbonaceous Particles and Polycyclic Aromatic Hydrocarbons from Residential Coal Combustion in China, Environ. Sci. Technol., 39, 1861-1867, https://doi.org/10.1021/es0493650, 2005.

Chesselet, R., Fontugne, M., Buat Menard, P., Ezat, U., and Lambert, C. E.: The origin of particulate organic carbon in the marine atmosphere as indicated by its stable carbon isotopic composition, Geophys. Res. Lett., 8, 345-348, https://doi.org/10.1029/GL008i004p00345, 1981.

Chow, J. C., and Watson, J. G.: PM2.5 carbonate concentrations at regionally representative Interagency Monitoring of Protected Visual Environment sites, Journal of Geophysical Research Atmospheres, 107, https://doi.org/10.1029/2001JD000574, 2002.

Chow, J. C., Watson, J. G., Chen, L. W. A., Arnott, W. P., Moosmüller, H., and Fung, K.: Equivalence of Elemental Carbon by Thermal/Optical Reflectance and Transmittance with Different Temperature Protocols, Environ. Sci. Technol., 38, 4414-4422, https://doi.org/10.1021/es034936u, 2004.

Claeys, M., Kourtchev, I., Pashynska, V., Vas, G., Vermeylen, R., Wang, W., Cafmeyer, J., Chi, X., Artaxo, P., Andreae, M. O., and Maenhaut, W.: Polar organic marker compounds in atmospheric aerosols during the LBA-SMOCC 2002 biomass burning experiment in Rondônia, Brazil: sources and source processes, time series, diel variations and size distributions, Atmos. Chem. Phys., https://doi.org/10.5194/acp-10-9319-2010, 2010.

Clarke, A. G., and Karani, G. N.: Characterisation of the carbonate content of atmospheric aerosols, J. Atmos. Chem., 14, 119-128, https://doi.org/10.1007/BF00115228, 1992.

Clayton, G. D., Arnold, J. R., and Patty, F. A.: Determination of Sources of Particulate

833 Atmospheric Carbon, Science, 122, 751-753,
834 https://doi.org/10.1126/science.122.3173.751, 1955.
835 Coplen, T. B.: New guidelines for reporting stable hydrogen, carbon, and oxygen
836 isotope-ratio data, Geochim. Cosmochim. Acta, 60, 3359-3360,
837 https://doi.org/10.1016/0016-7037(96)00263-3, 1996.
838 CSC: (Chinese State Council): Action Plan for Air Pollution Prevention and Control,
839 http://www.gov.cn/zhengce/content/2013-09/13/content_4561.htm, 2013 (last
840 access: 28 March 2022).
841 CSC: (Chinese State Council): Three-year action plan to fight air pollution (NO. 2018.
842 22), http://www.gov.cn/zhengce/content/2018-07/03/content_5303158.htm, 2018
843 (last access: 28 March 2022).
844 Currie, L. A.: Evolution and Multidisciplinary Frontiers of 14C Aerosol Science,
845 Radiocarbon, 42, 115-126, https://doi.org/10.1017/S003382220005308X, 2000.
846 Draxler, R. R., and Hess, G. D.: An overview of the HYSPLIT_4 modelling system
847 for trajectories, dispersion and deposition, Aust. Meteorol. Mag., 47, 295-308,
848 1998.
849 England, G., Chang, O., and Wien, S.: Development of fine particulate emission
850 factors and speciation profiles for oil and gas-fired combustion systems, United
851 States, 2002.
852 Engling, G., Carrico, C. M., Kreidenweis, S. M., CollettJr., J. L., Day, D. E., Malm, W.
853 C., Lincoln, E., Hao, W. M., Iinuma, Y., and Herrmann, H.: Determination of
854 levoglucosan in biomass combustion aerosol by high-performance
855 anion-exchange chromatography with pulsed amperometric detection, Atmos.
856 Environ., 2006,40, S299-S311, https://doi.org/10.1016/j.atmosenv.2005.12.069,
857 2006.

858 Engling, G., Lee, J. J., Tsai, Y. W., Lung, S. H., C., C., Chou, C. K., and Chan, C.:
859 Size-Resolved Anhydrosugar Composition in Smoke Aerosol from Controlled
860 Field Burning of Rice Straw, Aerosol Sci. Technol., 43, 662-672,
861 https://doi.org/10.1080/02786820902825113, 2009.
862 Fang, W., Andersson, A., Zheng, M., Lee, M., Holmstrand, H., Kim, S. W., Du, K.,
863 and Örjan, G.: Divergent Evolution of Carbonaceous Aerosols during Dispersal
864 of East Asian Haze, Sci. Rep., 7, 10422,
865 https://doi.org/10.1038/s41598-017-10766-4, 2017.
866 Feng, Y. L., Chen, Y. J., Guo, H., Zhi, G. R., Xiong, S. C., Li, J., Sheng, G. Y., and Fu,
867 J. M.: Characteristics of organic and elemental carbon in PM2.5 samples in
868 Shanghai, China, Atmos. Res., 92, 434-442,
869 https://doi.org/10.1016/j.atmosres.2009.01.003, 2009.
870 Fu, P. Q., Kawamura, K., Chen, J., Li, J., Sun, Y. L., Liu, Y., Tachibana, E., Aggarwal,
871 S. G., Okuzawa, K., Tanimoto, H., Kanaya, Y., and Wang, Z. F.: Diurnal
872 variations of organic molecular tracers and stable carbon isotopic composition in
873 atmospheric aerosols over Mt. Tai in the North China Plain: an influence of
874 biomass burning, Atmos. Chem. Phys., 12, 8359–8375,
875 https://doi.org/10.5194/acp-12-8359-2012, 2012.
876 Gao, J. J., Wang, K., Wang, Y., Liu, S. H., Zhu, C. Y., Hao, J. M., Liu, H. J., Hua, S.
877 B., and Tian, H. Z.: Temporal-spatial characteristics and source apportionment of
878 PM2.5 as well as its associated chemical species in the Beijing-Tianjin-Hebei
879 region of China, Environ. Pollut., 233, 714-724,
880 https://doi.org/10.1016/j.envpol.2017.10.123, 2018.
881 Gelencsér, A., May, B., Simpson, D., Sánchez-Ochoa, A., Kasper-Giebl, A., Puxbaum,
882 H., Caseiro, A., Pio, C., and Legrand, M.: Source apportionment of PM2.5

883 organic aerosol over Europe: Primary/secondary, natural/anthropogenic, and
884 fossil/biogenic origin, J. Geophys. Res.: Atmos., 112,
885 https://doi.org/10.1029/2006jd008094, 2007.
886 Genberg, J., Hyder, M., Stenström, K., Bergström, R., Simpson, D., Fors, E. O.,
887 Jönsson, J. A., and Swietlicki, E.: Source apportionment of carbonaceous aerosol
888 in southern Sweden, Atmos. Chem. Phys., 11, 13575-13616,
889 https://doi.org/10.5194/acp-11-11387-2011, 2011.
890 Guo, J. D., Ge, Y. S., Hao, L. J., Tan, J. W., Li, J. Q., and Feng, X. Y.: On-road
891 measurement of regulated pollutants from diesel and CNG buses with urea
892 selective catalytic reduction systems, Atmos. Environ.,
893 https://doi.org/10.1016/j.atmosenv.2014.07.032, 2014.
894 Hammer, S., and Levin, I.: Monthly mean atmospheric D14CO2 at Jungfraujoch and
895 Schauinsland from 1986 to 2016, Tellus B, 65, 20092,
896 https://doi.org/10.11588/data/10100, 2017.
897 Han, R., Wang, S. X., Shen, W. H., Wang, J. D., Wu, K., Ren, Z. H., and Feng, M. N.:
898 Spatial and temporal variation of haze in China from 1961 to 2012, J. Environ.
899 Sci., 46, 1001-0742, https://doi.org/10.1016/j.jes.2015.12.033, 2016a.
900 Han, Y. M., Chen, L. W., Huang, R. J., Chow, J. C., Watson, J. G., Ni, H. Y., Liu, S. X.,
901 Fung, K. K., Shen, Z. X., Wei, C., Wang, Q. Y., J.Tian, Zhao, Z. Z., Prévôt, A. S.
902 H., and Cao, J. J.: Carbonaceous aerosols in megacity Xi'an, China: Implications
903 of thermal/optical protocols comparison, Atmos. Environ.,
904 https://doi.org/10.1016/j.atmosenv.2016.02.023, 2016b.
905 Heal, M. R.: The application of carbon-14 analyses to the source apportionment of
906 atmospheric carbonaceous particulate matter: a review, Anal. Bioanal. Chem.,
907 406, 81–98, https://doi.org/10.1007/s00216-013-7404-1, 2014.

908 Ho, K. F., Lee, S. C., Cao, J. J., Li, Y. S., Chow, J. C., Watson, J. G., and Fung, K.:
909 Variability of organic and elemental carbon, water soluble organic carbon, and
910 isotopes in Hong Kong, Atmos. Chem. Phys., 6, 4569–4576,
911 https://doi.org/10.5194/acp-6-4569-2006, 2006.
912 Hoffmann, D., Tilgner, A., Iinuma, Y., and Herrmann, H.: Atmospheric stability of
913 levoglucosan: a detailed laboratory and modeling study, Environ. Sci. Technol.,
914 44, 694-699, https://doi.org/10.1021/es902476f, 2010.
915 Hoyle, C. R., Boy, M., Donahue, N. M., Fry, J. L., Glasius, M., Guenther, A., Hallar,
916 A. G., Hartz, K. H., Petters, M., Petäjä, T., Rosenoern, T., and Sullivan, A. P.: A
917 review of the anthropogenic influence on biogenic secondary organic aerosol,
918 Atmos. Chem. Phys., 11, https://doi.org/10.5194/acp-11-321-2011, 2011.
919 Hua, Q., and Barbetti, M.: Review of Tropospheric Bomb 14C Data for Carbon Cycle
920 Modeling and Age Calibration Purposes, Radiocarbon, 46,
921 https://doi.org/10.1017/S0033822200033142, 2004.
922 Huang, J., Kang, S. C., Shen, C. D., Cong, Z. Y., Liu, K. X., Wang, W., and Liu, L. C.:
923 Seasonal variations and sources of ambient fossil and biogenic-derived
924 carbonaceous aerosols based on 14C measurements in Lhasa, Tibet, Atmos. Res.,
925 96, 553-559, https://doi.org/10.1016/j.atmosres.2010.01.003, 2010.
926 Huang, L., Brook, J. R., Zhang, W., Li, S. M., Graham, L., Ernst, D., Chivulescu, A.,
927 and Lu, G.: Stable isotope measurements of carbon fractions (OC/EC) in
928 airborne particulate: A new dimension for source characterization and
929 apportionment, Atmos. Environ., 40, 2690-2705,
930 https://doi.org/10.1016/j.atmosenv.2005.11.062, 2006.
931 Huang, R. J., Zhang, Y. L., Bozzetti, C., Ho, K. F., Cao, J. J., Han, Y. M., Dällenbach,
932 K. R., Slowik, J. G., Platt, S. M., Canonaco, F., Zotter, P., Wolf, R., Pieber, S. M.,

933 Bruns, E. A., Crippa, M., Ciarelli, G., Piazzalunga, A., Schwikowski, M.,
934 Abbaszade, G., Schnelle-Kreis, J., Zimmermann, R., An, Z., Szidat, S.,
935 Baltensperger, U., Haddad, I. E., and Prévôt, A.: High secondary aerosol
936 contribution to particulate pollution during haze events in China, Nature, 514,
937 218-222, https://doi.org/10.1038/nature13774, 2014.
938 Jacobson, M. C., Hansson, H.-C., Noone, K. J., and Charlson, R. J.: Organic
939 atmospheric aerosols: Review and state of the science, Rev. Geophys., 38,
940 267-294, https://doi.org/10.1029/1998RG000045, 2000.
941 Jacobson, M. Z.: Strong radiative heating due to the mixing state of black carbon in
942 atmospheric aerosols, Nature, https://doi.org/10.1038/35055518, 2001.
943 Ji, D. S., Yan, Y. C., Wang, Z. S., He, J., Liu, B. X., Sun, Y., Gao, M., Li, Y., Cao, W.,
944 Cui, Y., Hu, B., Xin, J. Y., Wang, L. L., Liu, Z. R., Tang, G. Q., and Wang, Y. S.:
945 Two-year continuous measurements of carbonaceous aerosols in urban Beijing,
946 China: Temporal variations, characteristics and source analyses, Chemosphere,
947 200, 191-200, https://doi.org/10.1016/j.chemosphere.2018.02.067, 2018.
948 Jimenez, J. L., Canagaratna, M. R., Donahue, N. M., Prevot, A. S. H., Zhang, Q.,
949 Kroll, J. H., DeCarlo, P. F., Allan, J. D., Coe, H., Ng, N. L., Aiken, A. C.,
950 Docherty, K. S., Ulbrich, I. M., Grieshop, A. P., Robinson, A. L., Duplissy, J.,
951 Smith, J. D., Wilson, K. R., Lanz, V. A., Hueglin, C., Sun, Y. L., Tian, J.,
952 Laaksonen, A., Raatikainen, T., Rautiainen, J., Vaattovaara, P., Ehn, M., Kulmala,
953 M., Tomlinson, J. M., Collins, D. R., Cubison, M. J., Dunlea, J., Huffman, J. A.,
954 Onasch, T. B., Alfarra, M. R., Williams, P. I., Bower, K., Kondo, Y., Schneider, J.,
955 Drewnick, F., Borrmann, S., Weimer, S., Demerjian, K., Salcedo, D., Cottrell, L.,
956 Griffin, R., Takami, A., Miyoshi, T., Hatakeyama, S., Shimono, A., Sun, J. Y.,
957 Zhang, Y. M., Dzepina, K., Kimmel, J. R., Sueper, D., Jayne, J. T., Herndon, S.

C., Trimborn, A. M., Williams, L. R., Wood, E. C., Middlebrook, A. M., Kolb, C. E., Baltensperger, U., and Worsnop, D. R.: Evolution of Organic Aerosols in the Atmosphere, Science, 326, 1525-1529, https://doi.org/10.1126/science.1180353, 2009.

Jull, A. J. T.: Radiocarbon dating| AMS method, in: Encyclopedia of Quaternary science 2911-2918, 2007.

Kawashima, H., and Haneishi, Y.: Effects of combustion emissions from the Eurasian continent in winter on seasonal δ13C of elemental carbon in aerosols in Japan, Atmos. Environ., 46, 568-579, https://doi.org/10.1016/j.atmosenv.2011.05.015, 2012.

Kiehl, J.: Twentieth century climate model response and climate sensitivity, Geophys. Res. Lett., 34, 22710, https://doi.org/10.1029/2007GL031383, 2007.

Kirillova, E. N., Andersson, A., Sheesley, R. J., Krusa, M., Praveen, P. S., Budhavant, K., Safai, P. D., Rao, P., and Gustafsson, Ö.: 13C- And 14C-based study of sources and atmospheric processing of water-soluble organic carbon (WSOC) in South Asian aerosols, Journal of Geophysical Research Atmospheres, 118, 614-626, https://doi.org/10.1002/jgrd.50130, 2013.

Kumagai, K., Iijima, A., Shimoda, M., Saitoh, Y., Kozawa, K., Hagino, H., and Sakamoto, K.: Determination of Dicarboxylic Acids and Levoglucosan in Fine Particles in the Kanto Plain, Japan, for Source Apportionment of Organic Aerosols, Aerosol Air Qual. Res., 10, 282-291, https://doi.org/10.4209/aaqr.2009.11.0075, 2010.

Levin, I., Kromer, B., Schmidt, M., and Sartorius, H.: A novel approach for independent budgeting of fossil fuel CO2 over Europe by 14CO2 observations, Geophys. Res. Lett., 30, https://doi.org/10.1029/2003GL018477, 2003.

983 Levin, I., Naegler, T., Kromer, B., Diehl, M., Francey, R., Gomez Pelaez, A., Steele, P.,
984 Wagenbach, D., Weller, R., and Worthy, D.: Observations and modelling of the
985 global distribution and long-term trend of atmospheric 14CO2, Tellus B, 62,
986 26-46, https://doi.org/10.1111/j.1600-0889.2009.00446.x, 2010.
987 Lewis, C. W., Klouda, G. A., and Ellenson, W. D.: Radiocarbon measurement of the
988 biogenic contribution to summertime PM-2.5 ambient aerosol in Nashville, TN,
989 Atmos. Environ., 38, 6053-6061, https://doi.org/10.1016/j.atmosenv.2004.06.011,
990 2004.
991 Li, C. L., Bosch, C., Kang, S. C., Andersson, A., Chen, P. F., Zhang, Q. G., Cong, Z.
992 Y., Chen, B., Qin, D. H., and Gustafsson, Ö.: Sources of black carbon to the
993 Himalayan-Tibetan Plateau glaciers, Nat. Commun., 7, 12574,
994 https://doi.org/10.1038/ncomms12574, 2016.
995 Li, H. M., Yang, Y., Wang, H. L., Li, B. J., Wang, P. Y., Li, J. D., and Liao, H.:
996 Constructing a spatiotemporally coherent long-term PM2.5 concentration dataset
997 over China during 1980–2019 using a machine learning approach, Sci. Total
998 Environ., 765, 0048-9697, https://doi.org/10.1016/j.scitotenv.2020.144263,
999 2021a.
1000 Li, X. R., Wang, Y. S., Guo, X. Q., and Wang, Y. F.: Seasonal variation and source
1001 apportionment of organic and inorganic compounds in PM2.5 and PM10
1002 particulates in Beijing, China, J. Environ. Sci., 25, 741-750,
1003 https://doi.org/10.1016/S1001-0742(12)60121-1, 2013.
1004 Li, Y. M., Fu, T.-M., Yu, J. Z., Feng, X., Zhang, L. J., Chen, J., Boreddy, S. K. R.,
1005 Kawamura, K., Fu, P., Yang, X., Zhu, L., and Zeng, Z. Z.: Impacts of chemical
1006 degradation on the global budget of atmospheric levoglucosan and its use as a
1007 biomass burning tracer, Environ. Sci. Technol., 55, 5525-5536,

https://doi.org/10.1021/acs.est.0c07313, 2021b.

Liao, C. P., Wu, C. Z., Yan, y. J., and Huang, H. T.: Chemical elemental characteristics of biomass fuels in China, Biomass Bioenergy, 27, 119-130, https://doi.org/10.1016/j.biombioe.2004.01.002, 2004.

Lim, S., Yang, X., Lee, M., Li, G., Jeon, K., Lim, S. H., YangYang, X., Lee, M. H., Li, G., Gao, Y. G., Shang, X. N., Zhang, K., I.Czimczik, C., Xu, X. M., Min-SukBae, Moon, K.-J., and Jeon, K.: Fossil-driven secondary inorganic PM2.5 enhancement in the North China Plain: Evidence from carbon and nitrogen isotopes, Environ. Pollut., 266, 115163, https://doi.org/10.1016/j.envpol.2020.115163, 2020.

Liu, D., Li, J., Zhang, Y. L., Xu, Y., Liu, X., Ping, D., Shen, C. D., Chen, Y. J., Tian, C., and Zhang, G.: The Use of Levoglucosan and Radiocarbon for Source Apportionment of PM2.5 Carbonaceous Aerosols at a Background Site in East China, Environ. Sci. Technol., 47, https://doi.org/10.1021/es401250k, 2013.

Liu, J., Mo, Y., Li, J., Liu, D., Shen, C., Ding, P., Jiang, H., Cheng, Z., Zhang, X., and Tian, C.: Radiocarbon‐derived source apportionment of fine carbonaceous aerosols before, during, and after the 2014 Asia‐Pacific Economic Cooperation (APEC) summit in Beijing, China, J. Geophys. Res.: Atmos., 121, 4177-4187, https://doi.org/10.5194/acp-16-2985-2016, 2016a.

Liu, J. W., Li, J., Liu, D., Ding, P., Shen, C. D., Mo, Y. Z., Wang, X. M., Luo, C. L., Cheng, Z. N., Szidat, S., Zhang, Y. L., Chen, Y. J., and Zhang, G.: Source apportionment and dynamic changes of carbonaceous aerosols during the haze bloom-decay process in China based on radiocarbon and organic molecular tracer, Atmos. Chem. Phys., 16, 2985–2996, https://doi.org/10.5194/acp-16-2985-2016, 2016b.

1033 Liu, Y., Shao, M., Fu, L. L., Lu, S. H., Zeng, L. M., and Tang, D. G.: Source profiles
1034 of volatile organic compounds (VOCs) measured in China: Part I, Atmos.
1035 Environ., 42, 6247-6260, https://doi.org/10.1016/j.atmosenv.2008.01.070, 2008.
1036 Liu, Z. R., Hu, B., Liu, Q., Sun, Y., and Wang, Y. S.: Source apportionment of urban
1037 fine particle number concentration during summertime in Beijing, Atmos.
1038 Environ., 96, 359-369, https://doi.org/10.1016/j.atmosenv.2014.06.055, 2014.
1039 Locker, H. B.: The use of levoglucosan to assess the environmental impact of
1040 residential wood-burning on air quality, Hanover, NH (US); Dartmouth College,
1041 1988.
1042 Lopez-Veneroni, D.: The stable carbon isotope composition of PM2.5 and PM10 in
1043 Mexico City Metropolitan Area air, Atmos. Environ., 43, 4491-4502,
1044 https://doi.org/10.1016/j.atmosenv.2009.06.036, 2009.
1045 Lu, L., Tang, Y., Xie, J. S., and Yuan, Y. L.: The role of marginal agricultural
1046 land-based mulberry planting in biomass energy production, Renewable Energy,
1047 34, 1789-1794, https://doi.org/10.1016/j.renene.2008.12.017, 2009.
1048 Martinelli, L. A., Camargo, P. B., Lara, L., Victoria, R. L., and Artaxo, P.: Stable
1049 carbon and nitrogen isotopic composition of bulk aerosol particles in a C4 plant
1050 landscape of southeast Brazil, Atmos. Environ., 36, 2427-2432,
1051 https://doi.org/10.1016/S1352-2310(01)00454-X, 2002.
1052 MEE: (Ministry of Ecology and Environment of the People'’s Republic of China):
1053 Technical Regulation on Ambient Air Quality Index, China Environmental
1054 Science Press (HJ 633–2012),
1055 http://www.mee.gov.cn/ywgz/fgbz/bz/bzwb/jcffbz/201203/t20120302_224166.sh
1056 tml, 2012 (last access: 28 March 2022).
1057 MEE: (Ministry of Ecology and Environment of the People'’s Republic of China):

Bulletin of Ecology and Environment of the People's Republic of China 2013, http://www.mee.gov.cn/hjzl/sthjzk/zghjzkgb/201605/P020160526564730573906.pdf, 2014 (last access: 28 March 2022).

MEE: (Ministry of Ecology and Environment of the People'’s Republic of China): Bulletin of Ecology and Environment of the People's Republic of China 2018, http://www.mee.gov.cn/hjzl/sthjzk/zghjzkgb/201905/P020190619587632630618.pdf, 2019 (last access: 28 March 2022).

MEE: (Ministry of Ecology and Environment of the People'’s Republic of China): Bulletin of Ecology and Environment of the People's Republic of China 2019, http://www.mee.gov.cn/hjzl/sthjzk/zghjzkgb/202006/P020200602509464172096.pdf., 2020 (last access: 28 March 2022).

MEE: (Ministry of Ecology and Environment of the People'’s Republic of China): Bulletin of Ecology and Environment of the People's Republic of China 2020, http://www.mee.gov.cn/hjzl/sthjzk/zghjzkgb/202105/P020210526572756184785.pdf, 2021 (last access: 28 March 2022).

Mook, W. G., and Plicht, J. V. D.: Reporting 14C Activities and Concentrations, Radiocarbon, 41, 227-239, https://doi.org/10.1017/S0033822200057106, 1999.

Moura, J. M. S., Martens, C. S., Moreira, M. Z., Lima, R. L., Sampaio, I. C. G., Mendlovitz, H. P., and Menton, M. C.: Spatial and seasonal variations in the stable carbon isotopic composition of methane in stream sediments of eastern Amazonia, Tellus B, 60, 21-31, https://doi.org/10.1111/j.1600-0889.2007.00322.x, 2008.

NBS: (National bureau of statistics): China Statistical Yearbook-2019, China Statistics press http://www.stats.gov.cn/tjsj/ndsj/2019/indexch.htm, 2020 (last access: 28 March 2022).

NBS: (National bureau of statistics): China Statistical Yearbook-2020, China Statistics press, http://www.stats.gov.cn/tjsj/ndsj/2020/indexch.htm, 2021 (last access: 28 March 2022).

Ni, H. Y., Huang, R. J., Cao, J. J., Liu, W. G., Zhang, T., Wang, M., Meijer, H. A., and Dusek, U.: Source apportionment of carbonaceous aerosols in Xi'an, China: insights from a full year of measurements of radiocarbon and the stable isotope C-13, Atmos. Chem. Phys., https://doi.org/10.5194/acp-18-16363-2018, 2018.

Ni, H. Y., Huang, R. J., Cosijn, M. M., Yang, L., and Dusek, U.: Measurement report: dual-carbon isotopic characterization of carbonaceous aerosol reveals different primary and secondary sources in Beijing and Xi'an during severe haze events, Atmos. Chem. Phys., 20, 16041-16053, https://doi.org/10.5194/acp-20-16041-2020, 2020.

Niu, Z. C., Wang, S., Chen, J. S., Zhang, F. W., Chen, X. Q., He, C., Lin, L. F., Yin, L. Q., and Xu, L. L.: Source contributions to carbonaceous species in PM2.5 and their uncertainty analysis at typical urban, peri-urban and background sites in southeast China, Environ. Pollut., 181, 107-114, https://doi.org/10.1016/j.envpol.2013.06.006, 2013.

Niu, Z. C., Zhou, W. J., Cheng, P., Wu, S. G., Lu, X. F., Xiong, X. H., Du, H., and Fu, Y. C.: Observations of Atmospheric Δ~(14)CO_2 at the Global and Regional Background Sites in China: Implication for Fossil Fuel CO_2 Inputs, Environ. Sci. Technol., 50, 12122-12128, https://doi.org/10.1021/acs.est.6b02814, 2016.

Niu, Z. C., Feng, X., Zhou, W. J., Wang, P., Liu, Y., Lu, X. F., Du, H., Fu, Y. C., Li, M., Mei, R. C., Li, Q., and Cai, Q. F.: Tree-ring Δ 14 C time series from 1948 to 2018at a regional background site, China: Influences of atmospheric nuclear weapons tests and fossil fuel emissions, Atmos. Environ., 246,

https://doi.org/10.1016/j.atmosenv.2020.118156, 2021.

Novakov, T., Menon, S., Kirchstetter, T. W., Koch, D., and Hansen, J. E.: Aerosol organic carbon to black carbon ratios: Analysis of published data and implications for climate forcing, Journal of Geophysical Research Atmospheres, 110, https://doi.org/10.1029/2005JD005977, 2005.

Oros, D. R., and Simoneit, B. R. T.: Identification and emission factors of molecular tracers in organic aerosols from biomass burning Part 2. Deciduous trees, Appl. Geochem., 16, 1545-1565, https://doi.org/10.1016/s0883-2927(01)00022-1, 2001a.

Oros, D. R., and Simoneit, B. R. T.: Identification and emission factors of molecular tracers in organic aerosols from biomass burning Part 1. Temperate climate conifers, Appl. Geochem., 16, 1513-1544, https://doi.org/10.1016/s0883-2927(01)00021-x, 2001b.

PGHP: (The People's Government of Hebei Province): Hebei Economic Yearbook-2020, China Statistics press, http://tjj.hebei.gov.cn/hetj/tjnj/2020/indexch.htm, 2021 (last access: 28 March 2022).

Popovicheva, O. B., Kozlov, V. S., Engling, G., Diapouli, E., Persiantseva, N. M., Timofeev, M. A., Fan, T.-S., Saraga, D., and Eleftheriadis, K.: Small-scale study of siberian biomass burning: i. smoke microstructure, Aerosol Air Qual. Res., 15, 117-128, https://doi.org/10.4209/aaqr.2014.09.0206, 2014.

Pugliese, S. C., Murphy, J. G., Vogel, F., and Worthy, D.: Characterization of the d13C signatures of anthropogenic CO2 emissions in the Greater Toronto Area, Canada, Appl. Geochem., 83, 171-1800, https://doi.org/10.1016/j.apgeochem.2016.11.003, 2017.

1133 Puxbaum, H., Caseiro, A., Sánchez-Ochoa, A., Kasper-Giebl, A., Claeys, M.,
1134 Gelencsér, A., Legrand, M., Preunkert, S., and Pio, C.: Levoglucosan levels at
1135 background sites in Europe for assessing the impact of biomass combustion on
1136 the European aerosol background, J. Geophys. Res., 112, D23S05,
1137 https://doi.org/10.1029/2006jd008114, 2007.
1138 Rajput, P., Sarin, M. M., Rengarajan, R., and Singh, D.: Atmospheric polycyclic
1139 aromatic hydrocarbons (pahs) from post-harvest biomass burning emissions in
1140 the indo-gangetic plain: isomer ratios and temporal trends, Atmospheric
1141 Environment, 45, 6732-6740, https://doi.org/10.1016/j.atmosenv.2011.08.018,
1142 2011.
1143 SAPBS: (Shaanxi Provincial Bureau of Statistics): Shaanxi Statistical Yearbook-2020,
1144 China Statistics press, http://tjj.shaanxi.gov.cn/upload/n2020/indexch.htm, 2020
1145 (last access: 28 March 2022).
1146 Seinfeld, J. H., and Pandis, S. N.: Atmospheric Chemistry and Physics: From Air
1147 Pollution to Climate Change, Environ.: Sci. Policy Sustainable Dev., 1998.
1148 Shang, J., Khuzestani, R. B., Tian, J., Schauer, J. J., Hua, J., Zhang, Y., Cai, T., Fang,
1149 D., An, J., and Zhang, Y.: Chemical characterization and source apportionment of
1150 PM2.5 personal exposure of two cohorts living in urban and suburban Beijing,
1151 Environ. Pollut., https://doi.org/10.1016/j.envpol.2018.11.076, 2019.
1152 Shao, M., Li, J., and Tang, X.: The application of accelerator mass spectrometry
1153 (AMS) in the study of source identification of aerosols (in Chinese). Acta
1154 Scientiae Circumstantiae 16 (2), 130–141, 1996.
1155 Shen, G. F., Wang, W., Yang, Y. F., Zhu, C., Min, Y. J., Xue, M., Ding, J. N., Li, W.,
1156 Wang, B., Shen, H. Z., Wang, R., Wang, X. L., and Tao, S.: Emission factors and
1157 particulate matter size distribution of polycyclic aromatic hydrocarbons from

residential coal combustions in rural Northern China, Atmos. Environ., 44, 5237-5243, https://doi.org/10.1016/j.atmosenv.2010.08.042, 2010.

Shen, Z. X., Cao, J. J., Liu, S. X., Zhu, C. S., Wang, X., Zhang, T., Xu, H. M., and Hu, T. F.: Chemical Composition of PM10 and PM2.5 Collected at Ground Level and 100 Meters during a Strong Winter-Time Pollution Episode in Xi'an, China, J. Air Waste Manage. Assoc., https://doi.org/10.1080/10473289.2011.608619, 2011.

Simoneit, B. R. T., Schauer, J. J., Nolte, C. G., Oros, D. R., Elias, V. O., Fraser, M. P., Rogge, W. F., and Cass, G. R.: Levoglucosan, a tracer for cellulose in biomass burning and atmospheric particles, Atmos. Environ., 33, 173-182, https://doi.org/10.1016/S1352-2310(98)00145-9, 1999.

Simpson, D., Yttri, K. E., Klimont, Z., Kupiainen, K., Caseiro, A., Gelencsér, A., Pio, C., Puxbaum, H., and Legrand, M.: Modeling carbonaceous aerosol over Europe: Analysis of the CARBOSOL and EMEP EC/OC campaigns, Journal of Geophysical Research Atmospheres, 112, -, https://doi.org/10.1029/2006JD008158, 2007.

Slota, P. J., Jull, A. J. T., Linick, T. W., and Toolin, L. J.: Preparation of Small Samples for 14C Accelerator Targets by Catalytic Reduction of CO, Radiocarbon, 29, 303-306, https://doi.org/10.1017/S0033822200056988, 1987.

Smith, B. N., and Epstein, S.: Two Categories of 13C/12C Ratios for Higher Plants, Plant Physiol., 47, 380-384, https://doi.org/10.1029/2006JD008158, 1971.

Song, Y., Zhang, Y. H., Xie, S. D., Zeng, L. M., Zheng, M., Salmon, L., Shao, M., and Slanina, S.: Source apportionment of PM2.5 in Beijing by positive matrix factorization, Atmos. Environ., 40, 1526-1537, https://doi.org/10.1016/j.atmosenv.2005.10.039, 2006.

SPBS: (Shanxi Provincial Bureau of Statistics): Shanxi Statistical Yearbook-2019, China Statistics press, http://tjj.shaanxi.gov.cn/upload/2020/pro/3sxtjnj/zk/indexch.htm, 2020 (last access: 28 March 2022).

Streets, D. G., Bond, T. C., Carmichael, G. R., Fernandes, S. D., Fu, Q., He, D., Klimont, Z., Nelson, S. M., Tsai, N. Y., Wang, M. Q., Woo, J. H., and Yarber, K. F.: An inventory of gaseous and primary aerosol emissions in Asia in the year 2000, J. Geophys. Res.: Atmos., 108, https://doi.org/10.1029/2002JD003093, 2003a.

Streets, D. G., Yarber, K. F., Woo, J.-H., and Carmichael, G. R.: Biomass burning in Asia: Annual and seasonal estimates and atmospheric emissions, Global Biogeochem. Cycles, 17, 1099, https://doi.org/10.1029/2003GB002040, 2003b.

Stuiver, M., and Polach, H.: Discussion: Reporting of 14C data, Radiocarbon, 19, 355-363, https://doi.org/10.1017/S0033822200003672, 1977.

Sun, X. S., Hu, M., Guo, S., Liu, K. X., and Zhou, L. P.: 14 C-Based source assessment of carbonaceous aerosols at a rural site, Atmos. Environ., 50, 36-40, https://doi.org/10.1016/j.atmosenv.2012.01.008, 2012.

Sun, Y. L., Zhuang, G. S., Tang, A. H., Wang, Y., and An, Z. S.: Chemical characteristics of PM2.5 and PM10 in haze-fog episodes in Beijing, Environ. Sci. Technol., 40, 3148-3155, https://doi.org/10.1021/es051533g, 2006.

Szidat, S., Jenk, T. M., Gaeggeler, H. W., Synal, H. A., Hajdas, I., Bonani, G., and Saurer, M.: THEODORE, a two-step heating system for the EC/OC determination of radiocarbon (14C) in the environment, Nucl. Instrum. Methods Phys. Res., 223, 829-836, https://doi.org/10.1016/j.nimb.2004.04.153, 2004.

Szidat, S., Jenk, T. M., Synal, H., Kalberer, M., Wacker, L., Hajdas, I., Kasper‐Giebl,

A., and Baltensperger, U.: Contributions of fossil fuel, biomass burning, and biogenic emissions to carbonaceous aerosols in Zürich as traced by 14C, Journal of Geophysical Research Atmospheres, 111, -, http://doi.org/10.1029/2005JD006590, 2006.

Szidat, S., Ruff, M., Perron, N., Wacker, L., Synal, H. A., Hallquist, M., Shannigrahi, A. S., Yttri, K., Dye, C., and Simpson, D.: Fossil and non-fossil sources of organic carbon (OC) and elemental carbon (EC) in Göteborg, Sweden, Atmos. Chem. Phys., 9, 16255-16289, https://doi.org/10.5194/acpd-8-16255-2008, 2009.

Tanarit, S., Alex, G., Detlev, H., Jana, M., and Christine, W.: Secondary Organic Aerosol from Sesquiterpene and Monoterpene Emissions in the United States, Environ. Sci. Technol., 42, 8784–8790, https://doi.org/10.1021/es800817r, 2008.

Tian, S. L., Pan, Y. P., and Wang, Y. S.: Size-resolved source apportionment of particulate matter in urban Beijing during haze and non-haze episodes, Atmos. Chem. Phys., 16, 9405-9443, https://doi.org/10.5194/acp-16-1-2016, 2016.

Turekian, V. C., Macko, S., Ballentine, D., Swap, R. J., and Garstang, M.: Causes of bulk carbon and nitrogen isotopic fractionations in the products of vegetation burns: laboratory studies, Chem. Geol., 152, 181-192, https://doi.org/10.1016/S0009-2541(98)00105-3, 1998.

Turnbull, J. C., Lehman, S. J., Miller, J. B., Sparks, R. J., Southon, J. R., and Tans, P. P.: A new high precision14CO2time series for North American continental air, J. Geophys. Res., http://doi.org/10.1029/2006jd008184, 2007.

Turpin, B. J., and Huntzicker, J. J.: Identification of secondary organic aerosol episodes and quantitation of primary and secondary organic aerosol concentrations during SCAQS, Atmos. Environ., 29, 3527-3544, https://doi.org/10.1016/1352-2310(94)00276-Q, 1995.

1233 Vardag, S. N., Gerbig, C., Janssens-Maenhout, G., and Levin, I.: Estimation of
1234 continuous anthropogenic CO2: model-based evaluation of CO2, CO,
1235 D13C(CO2) and D14C(CO2) tracer methods, Atmos. Chem. Phys., 15,
1236 12705–12729, https://doi.org/10.5194/acp-15-12705-2015, 2015.
1237 Vonwiller, M., Quintero, G. S., and Szidat, S.: Isolation and 14C analysis of
1238 humic-like substances (HULIS) from ambient aerosol samples,
1239 https://doi.org/10.7892/boris.108864, 2017.
1240 Wang, G., Cheng, S., Li, J., Lang, J., Wen, W., Yang, X., Tian, L., Wang, G., Cheng, S.
1241 Y., Li, J. B., Lang, J. L., Wen, W., Yang, X. W., and Tian, L.: Source
1242 apportionment and seasonal variation of PM2.5 carbonaceous aerosol in the
1243 Beijing-Tianjin-Hebei Region of China, Environ. Monit. Assess., 187, 1-13,
1244 https://doi.org/10.1007/s10661-015-4288-x, 2015.
1245 Wang, H. L., Zhuang, Y. H., Wang, Y., Yuan, Y. L., and Zhuang, G. S.: Long-term
1246 monitoring and source apportionment of PM2.5/PM10 in Beijing, China, J.
1247 Environ. Sci., 20, 1323-1327, https://doi.org/10.1016/S1001-0742(08)62228-7,
1248 2008.
1249 Wang, X. F., Zhu, G. H., Wu, Y. G., and Shen, X. Y.: Chemical composition and size
1250 distribution of particles in the atmosphere in north part of Beijing city for winter
1251 and summer (In Chinese), Chinese Journal of Atmospheric Sciences, 14, 199-206,
1252 https://doi.org/10.3878/j.issn.1006-9895.1990.02.09, 1990.
1253 Wang, Z. Z., Bi, X. H., Sheng, G. Y., and Fu, J. M.: Characterization of organic
1254 compounds and molecular tracers from biomass burning smoke in South China I:
1255 Broad-leaf trees and shrubs, Atmos. Environ., 43, 3096-3102,
1256 https://doi.org/10.1016/j.atmosenv.2009.03.012, 2009.
1257 Weber, R. J., Sullivan, A. P., Peltier, R. E., Russell, A., Yan, B., Zheng, M., Gouw, J.

1258 D., Warneke, C., Brock, C., and Holloway, J. S.: A study of secondary organic
1259 aerosol formation in the anthropogenic-influenced southeastern United States,
1260 Journal of Geophysical Research Atmospheres, 112, D13302,
1261 https://doi.org/10.1029/2007jd008408, 2007.
1262 Widory, D.: Combustibles, fuels and their combustion products: A view through
1263 carbon isotopes, Combust. Theor. Model., 10, 831-841,
1264 https://doi.org/10.1080/13647830600720264, 2006.
1265 Winiger, P., Andersson, A., Eckhardt, S., Stohl, A., Semiletov, I. P., Dudarev, O. V.,
1266 Charkin, A., Shakhova, N., Klimont, Z., and Heyes, C.: Siberian Arctic black
1267 carbon sources constrained by model and observation, Proc Natl Acad Sci U S A,
1268 114, E1054, https://doi.org/10.1073/pnas.1613401114, 2017.
1269 Wu, J., Kong, S. F., Zeng, X., Cheng, Y., Yan, Q., Zheng, H., Yan, Y. Y., Zheng, S. R.,
1270 Liu, D. T., Zhang, X. Y., Fu, P. Q., Wang, S. X., and Qi, S. H.: First
1271 High-Resolution Emission Inventory of Levoglucosan for Biomass Burning and
1272 Non-Biomass Burning Sources in China, Environ. Sci. Technol., 55, 1497-1507,
1273 https://doi.org/10.1021/acs.est.0c06675, 2021.
1274 XAMBS: (Xi'an Municipal Bureau Statistics): Xi'an Statistical Yearbook-2014,
1275 China Statistics press, http://tjj.xa.gov.cn/tjnj/2014/tjnj/indexch.htm, 2014 (last
1276 access: 28 March 2022).
1277 XAMBS: (Xi'an Municipal Bureau Statistics): Xi'an Statistical Yearbook-2020 China
1278 Statistics press, http://tjj.xa.gov.cn/tjnj/2020/zk/indexch.htm, 2021 (last access:
1279 28 March 2022).
1280 Yan, X. Y., Ohara, T., and Akimoto, H.: Bottom-up estimate of biomass burning in
1281 mainland china, Atmos. Environ., 40, 5262-5273,
1282 https://doi.org/10.1016/j.atmosenv.2006.04.040, 2006.

1283 Yan, X. Y., and Crookes, R. J.: Energy demand and emissions from road
1284 transportation vehicles in China, Prog. Energy Combust. Sci., 36, 651-676,
1285 https://doi.org/10.1016/j.pecs.2010.02.003, 2010.
1286 Yang, F., He, K., Ye, B., Chen, X., Cha, L., Cadle, S. H., Chan, T., and Mulawa, P. A.:
1287 One-year record of organic and elemental carbon in fine particles in downtown
1288 Beijing and Shanghai, Atmos. Chem. Phys., 5, 1449-1457,
1289 https://doi.org/10.5194/acp-5-1449-2005, 2005.
1290 Zhang, R., Jing, J., Tao, J., Hsu, S. C., Wang, G., Cao, J., Lee, C. S. L., Zhu, L., Chen,
1291 Z., and Zhao, Y.: Chemical characterization and source apportionment of PM2.5
1292 in Beijing: seasonal perspective, Atmos. Chem. Phys., 13, 7053-7074,
1293 https://doi.org/10.5194/acp-14-175-2014, 2014.
1294 Zhang, Y. L., Perron, N., Ciobanu, V. G., Zotter, P., and Szidat, S.: On the isolation of
1295 OC and EC and the optimal strategy of radiocarbon-based source apportionment
1296 of carbonaceous aerosols, Soil Biol. Biochem., 12, 17657-17702,
1297 https://doi.org/10.5194/acpd-12-17657-2012, 2012.
1298 Zhang, Y. L., Huang, R. J., Haddad, I. E. l., Ho, K. F., Cao, J. J., Han, Y., Zotter, P.,
1299 Bozzetti, C., Daellenbach, K. R., Canonaco, F., Slowik, J. G., Salazar, G.,
1300 Schwikowski, M., Schnelle-Kreis, J., Abbaszade, G., Zimmermann, R.,
1301 Baltensperger, U., Pr évôt, A. S. H., and Szidat, S.: Fossil vs. non-fossil sources
1302 of fine carbonaceous aerosols in four Chinese cities during the extreme winter
1303 haze episode of 2013, Atmos. Chem. Phys., 15, 1299-1312,
1304 https://doi.org/10.5194/acp-15-1299-2015, 2015.
1305 Zhang, Y. l., Ren, H., Sun, Y. L., Cao, F., Chang, Y. H., Liu, S. D., Lee, X. H., Agrios,
1306 K., Kawamura, K., Liu, D., Ren, L. J., Du, W., Wang, Z. F., Pr évôt, A. S. H.,
1307 Szidat§, S., and Fu, P. Q.: High Contribution of Nonfossil Sources to

1308 Submicrometer Organic Aerosols in Beijing, China, Environ. Sci. Technol., 51,
1309 7842, https://doi.org/10.1021/acs.est.7b01517, 2017a.
1310 Zhang, Y. X., Shao, M., Zhang, Y. H., Zeng, L. M., HE., L. Y., Zhu, B., Wei, Y. J., and
1311 Zhu, X. L.: Source profiles of particulate organic matters emitted from cereal
1312 straw burnings, J. Environ. Sci., 19, 167-175,
1313 https://doi.org/10.1016/S1001-0742(07)60027-8, 2007.
1314 Zhang, Z. S., Engling, G., Chan, C. Y., Yang, Y. H., Lin, M., Shi, S., He, J., Li, Y. D.,
1315 and Wang, X. M.: Determination of isoprene-derived secondary organic aerosol
1316 tracers (2-methyltetrols) by HPAEC-PAD: Results from size-resolved aerosols in
1317 a tropical rainforest, Atmos. Environ., 70, 468-476,
1318 https://doi.org/10.1016/j.atmosenv.2013.01.020, 2013.
1319 Zhang, Z. S., Gao, J., Zhang, L. M., Wang, H., Tao, J., Qiu, X. H., Chai, F. H., Li, Y.,
1320 and Wang, S. L.: Observations of biomass burning tracers in pm 2.5 at two
1321 megacities in north china during 2014 apec summit, Atmos. Environ., 169, 54-65,
1322 http://dx.doi.org/10.1016/j.atmosenv.2017.09.011, 2017b.
1323 Zhao, P. S., Dong, F., Yang, Y. D., He, D., Zhao, X. J., Zhang, W. Z., Yao, Q., and Liu,
1324 H. Y.: Characteristics of carbonaceous aerosol in the region of Beijing, Tianjin,
1325 and Hebei, China, Atmos. Environ., 71, 389–398,
1326 https://doi.org/10.1016/j.atmosenv.2013.02.010, 2013.
1327 Zhao, Z. Z., Cao, J. J., Zhang, T., XingShen, Z., Ni, H. Y., Tian, J., Wang, Q. Y., Liu, S.
1328 X., Zhou, J. M., Gu, J., and Shen, G. Z.: Stable carbon isotopes and levoglucosan
1329 for pm 2.5 elemental carbon source apportionments in the largest city of
1330 northwest china, Atmos. Environ., 185, 253-261,
1331 https://doi.org/10.1016/j.atmosenv.2018.05.008, 2018.
1332 Zhi, G. R., Chen, Y. J., Feng, Y. L., Xiong, S. C., Jun, L. I., Zhang, G., Sheng, G. Y.,

and Jiamo, F. U.: Emission characteristics of carbonaceous particles from various residential coal-stoves in China, Environ. Sci. Technol., 42, 3310, https://doi.org/10.1021/es702247q, 2008.

Zhou, W. J., Zhao, X. L., Feng, L. X., Lin, L., Kun, W. Z., Peng, C., Nian, Z. W., and Hai, H. C.: The 3MV multi-element AMS in Xi'an, China: Unique features and preliminary tests, Radiocarbon, 48, 285-293, https://doi.org/10.1017/S0033822200066492, 2006.

Zhou, W. J., Lua, X. F., Wu, Z. K., Zhao, W. N., Huang, C. H., Lia, L. L., Chen, P., and Xin, Z. H.: New results on Xi'an-AMS and sample preparation systems at Xi'an-AMS center, Nucl. Instrum. Methods Phys. Res., 262, 135-142, https://doi.org/10.1016/j.nimb.2007.04.221, 2007.

Zhou, W. J., Wu, S. G., Huo, W. W., Xiong, X. H., Cheng, P., Lu, X. F., and Niu, Z. C.: Tracing fossil fuel CO2 using Δ14C in Xi'an City, China, Atmos. Environ., 94, 538-545, https://doi.org/10.1017/S0033822200066492, 2014.